vcccar
victorian centre for climate change adaptation research

Technical Report

A multi-scale assessment of urban heating in Melbourne during an extreme heat event: policy approaches for adaptation

Andrew Coutts and Richard Harris
School of Geography and Environmental Science

Monash University

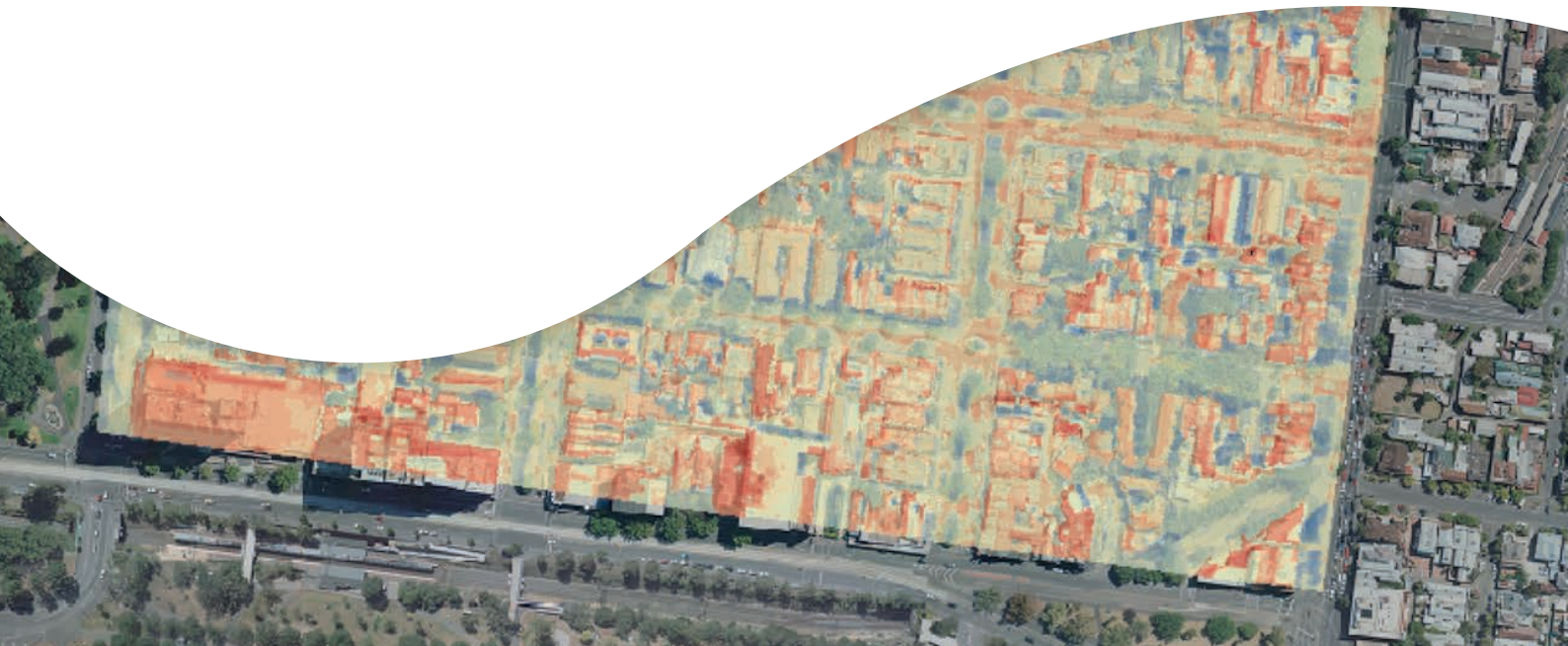

November 2012

A report for the Victorian Centre for Climate Change Adaptation Research (VCCCAR) under the project: Responding to the urban heat island: Optimising the implementation of green infrastructure.

This paper was prepared by Andrew Coutts and Richard Harris from the School of Geography and Environmental Science at Monash University.

For citation purposes: Coutts A, Harris R 2013. Urban Heat Island Report: *A multi-scale assessment of urban heating in Melbourne during an extreme heat event: policy approaches for adaptation,* Victorian Centre for Climate Change Adaptation Research

Contents

Executive Summary

Airborne thermal remote sensing can provide an excellent snapshot of spatial variability in land surface temperatures across the urban landscape. This can be used to broadly identify hot-spots across the landscape for prioritising the implementation of excess heat mitigation measures such as green infrastructure. Thermal mapping is an excellent tool for communicating the influence of urban design on urban climate and can help guide sustainable urban development. This report assesses both the influence of green infrastructure on land surface temperatures, and provides an assessment of the practical application of high resolution airborne thermal remote sensing for policy development targeting excess heat mitigation.

Drawing primarily on airborne thermal remote sensing data collected during an extreme heat event in Melbourne in February 2012, this study assessed the role of different urban land surface types and design on land surface temperatures in two study areas in the City of Port Phillip (CoPP) and the City of Melbourne (CoM). Complementary data was also drawn from satellite remote sensing and ground based thermography.

Findings

1. Increasing overall vegetation cover was effective at reducing land surface temperatures during the extreme heat event during both the day and night. During the day, tree cover and irrigated grass were particularly effective at reducing land surface temperatures, while at night, grass surfaces (irrigated and non-irrigated) were most effective. Under the study conditions for the CoPP study area, a 10 per cent increase in total vegetation cover resulted in a 1°C reduction in land surface temperature during the day.

2. Detailed analysis of the thermal images determined that green infrastructure should be prioritised to maximise daytime shading of the land surface. Street trees, green roofs and green walls can reduce daytime surface temperatures if designed well and strategically placed.

3. Data on air temperatures revealed that patterns of land surface temperature and air temperature were similar. Therefore, thermal remote sensing can be used as a proxy for spatial differences in urban heating and identifying hot-spots.

4. There was no clear relationship between absolute air temperatures and thermal remote sensing and therefore in the magnitude of differences in air temperatures between different locations.

While high resolution airborne thermal remote sensing can provide a means of identifying hot-spots in the landscape, there are some important features that limit its practical application.

Airborne thermal remote sensing produces a land surface temperature derived from surface irradiance. If absolute surface temperatures are required, an emissivity (relative power of a surface to emit heat by radiation) correction must be made. Without high resolution, high quality data such as hyper-spectral land surface data with which to identify individual land surface types, an emissivity correction is extremely difficult and is a major limitation of this data source.

Airborne thermal remote sensing provides a biased plan view of surface temperature for what is actually a complex 3D urban morphology. It therefore neglects important surface temperatures (e.g. walls) that also have a major influence on urban climates. Despite the excellent spatial coverage of airborne thermal remote sensing, the temporal coverage is poor and could lead to bias in interpretation due to the particular solar and meteorological conditions at the time of collection. Finally, the usefulness of airborne thermal remote sensing is heavily dependent on the quality of the data and auxiliary data used for interpretation.

The project has added significant value to the airborne thermal remote sensing data acquired by local councils. The ground based monitoring of surface temperatures enabled a validation of the thermal imagery in the case of CoPP and identified that the quality of the image was acceptable. The project also produced a new thermal image of surface temperatures corrected for emissivity across the CoPP municipality. In the

case of CoM, the ground based monitoring stations allowed the assignment of surface temperature values to the digital numbers captured by the thermal camera.

Overall, this study has demonstrated that increasing vegetation throughout the landscape is an effective approach for reducing land surface temperatures and the practical application of airborne thermal remote sensing for policy development concerning green infrastructure implementation. However, with regards to using high resolution airborne thermal remote sensing as a tool, issues around quality data collection and post-processing make the approach questionable, depending on its intended use. If broad surface temperature patterns are all that is required for identifying hot spots, then a raw thermal image will suffice. If a rigorous thermal image is needed for detailed analysis, then hyper-spectral data should be collected inclusive of the thermal bands, to provide a higher quality product and potential for emissivity correction, although this approach will increase the cost of collection and post-collection processing.

An alternative to high resolution airborne thermal mapping includes the use of coarser but more accessible satellite thermal remote sensing such as Landsat ETM for identifying hot-spots. This can be used in combination with the broad guidance on green infrastructure implementation provided in this study to target areas of high heat exposure to improve urban climates.

This report and other products produced from the VCCCAR project have provided valuable information on the effectiveness of urban greening and provide advice on approaches to green infrastructure implementation. Councils may wish to map areas of high land surface temperatures within their own municipality. However, the results presented here are sufficient for councils to proceed with initial planning of greening programs, as it describes the situations that lead to excessive surface heating and how vegetation should be located to counter this effect. The Green Infrastructure Implementation Guide being developed as part of the project will provide further guidance on designing green infrastructure to reduce urban heating.

1. Introduction

Urban development drastically alters the land surface, converting natural landscapes of vegetation, soil and water to hard, impervious surfaces. This alters urban land surface – atmosphere interactions and leads to the development of distinct urban climates (Stone and Rodgers, 2001). At times, air temperatures in urban areas can be warmer than surrounding urban landscapes, particularly at night, a phenomenon known as the Urban Heat Island (UHI) effect. As a result, urban residents may be exposed to elevated air temperatures for longer periods of the day. McMichael et al., (2006) suggests that people living in urban environments are at a heightened risk of heat related illnesses due to the UHI effect.

Green infrastructure (GI) delivers a range of benefits within the urban environment. Vegetation can provide aesthetic pleasure for people, shading for communal activities and outdoor recreational activities, increased privacy, and habitats for wildlife (Brack, 2002). Shading from vegetation can reduce building energy consumption (Akbari and Konopacki, 2005) and with careful vegetation selection can improve air quality (Nowak et al., 2006). Green infrastructure can also help to minimise stormwater runoff while improving stormwater quality reaching receiving waters (Fletcher et al., 2008). Finally, green infrastructure can serve to limit urban heating (Rosenzweig et al., 2009) and help cities adapt to future climate change (Gill et al., 2007).

Green infrastructure increases evaporative cooling during the day, especially when water is available, resulting in reduced surface temperatures (Spronken-Smith et al., 2000). Green infrastructure (trees) also increases shading of urban surfaces (buildings, roads) so less heat is conducted into urban surfaces during the day for release at night to support urban warming (Wong et al., 2003). Trees are particularly effective in supporting urban cooling (Upmanis and Chen, 1999; Shashua-Bar and Hoffman, 2004). Finally, green infrastructure (green roofs and walls) can also act as an additional insulating layer, reducing heat transfer into buildings during the day and improving daytime energy efficiency of buildings (Liu and Minor, 2005; Niachou et al., 2001).

While there are many studies that demonstrate the benefits of vegetation for urban cooling, Bowler et al., (2010) state that:

> *The current evidence base does not allow specific recommendations to be made on how best to incorporate greening into an urban area. Further empirical research is necessary in order to efficiently guide the design and planning of urban green space, and specifically to investigate the importance of the abundance, distribution and type of greening.* (p. 147). While the benefits of green infrastructure are clear, there is little guidance on how to implement green infrastructure on the ground to maximise cooling benefits.

This study employs the use of airborne thermal remote sensing, along with additional data sources to assess the relative influence of surface types and urban arrangements on surface temperature and the effectiveness of greening for urban cooling. High resolution airborne thermal remote sensing has attracted interest recently as a tool for developing policy to address excessive urban heating that can result at times from urban development. Airborne thermal remote sensing provides a high resolution snapshot of surface irradiance, which can be converted to a spatial map of surface temperature. The intention is often to use these data to identify hot-spots, along with understanding urban arrangements that are conducive to the development of excessive urban temperatures. A key assumption in this approach is that street level air temperatures follow similar patterns to land surface temperature – although the magnitudes in air temperature differences will be reduced. Air temperatures are of most interest as research demonstrates relationships between air temperature and mortality (Nicholls et al., 2008) and the general public identifies best with air temperature.

In the summer of 2011-12, the City of Port Phillip and the City of Melbourne sought to undertake airborne thermal remote sensing of their municipalities. The Victorian Centre for Climate Change Adaptation Research (VCCCAR) facilitated the collaboration of these local councils with Monash University, the University of Melbourne and RMIT, to work with thermal imagery as part of a broader project on *Responding to the urban heat island: Optimising the implementation of green infrastructure*. The airborne thermal remote

sensing provided a good basis for undertaking a research project investigating relationships between land surface temperature and land surface characteristics such as vegetation cover and building geometry. This report focuses on the analysis and interpretation of the airborne thermal remote sensing and examines the drivers of high land surface temperatures in urban areas in a bid to support implementation of green infrastructure.

An earlier VCCCAR research report (Coutts et al., 2012) provided an extensive review (referred to as the Technical Report) on the application of high resolution airborne thermal remote sensing and it is necessary to reiterate here the main findings. An excerpt from the Executive Summary is provided below. It is recommended that the Technical Report be read in combination with this report as it provides more information concerning differences between the surface UHI and canopy layer UHI, along with details on the advantages and limitations of airborne thermal remote sensing. It is also recommended that anyone using the airborne thermal remote sensing data should read the Technical Report to gain an understanding of what the data truly provides.

A number of studies have drawn on high resolution airborne thermal remote sensing for analysis of surface temperatures in urban areas. Previous research using high resolution airborne thermal remote sensing has focused on understanding relationships between land surface temperature and land surface characteristics. Vegetation has a strong influence on land surface temperatures, with areas of high vegetation cover generally showing lower surface temperatures (Lo et al., 1997; Saaroni et al., 2000) due to both evaporative cooling effects (Quattrochi and Ridd, 1994) and shading (Kottmeier et al. 2007). Urban geometry has been shown to be a major controller of land surface temperatures (Bärring et al., 1985) with shading from buildings important in lowering surface temperatures during the day (Kottmeier et al. 2007) while night time surface temperatures have been shown to be higher in areas of low sky-view factor (degree to which the sky is obscured by the surroundings) (Eliasson, 1992).

This study aimed to understand the influence of land surface characteristics such as vegetation cover and urban geometry on land surface temperatures and the development of the urban heat island using high resolution airborne thermal remote sensing data. Key objectives of the study were to:

- examine relationships between land surface temperature, vegetation cover and urban morphology
- evaluate a methodology for undertaking high resolution airborne thermal remote sensing data and correcting airborne thermal remote sensing data for emissivity
- understand relationships between land surface temperature and air temperature in the context of mapping hot-spots
- consider the implications for urban planning and design drivers of urban climates in relation to future climate adaptation
- assess the value of airborne thermal remote sensing for urban planning and policy development.

The airborne thermal remote sensing data was collected in collaboration with local governments, who funded and led the collection of the data and provided it to the project. The VCCCAR project has added significant value to the captured airborne thermal remote sensing by local councils. The VCCCAR research team compiled a number of auxiliary datasets to help interpret and analyse the thermal imagery. This project is a result of collaboration between multiple research and government organisations aimed at delivering scientifically rigorous, policy relevant outcomes for future planning and action in response to excess urban heating.

Excerpt from the Technical Report

Airborne thermal remote sensing is an attractive option for identifying areas of high surface heat exposure, providing an idea of priority areas for green infrastructure implementation. Airborne thermal remote sensing gives an excellent spatial picture of the urban landscape for a snapshot in time, allowing a comparative analysis of areas of high surface temperatures. The advantage of airborne thermal remote sensing is the ability to observe high resolution (1-5 m) surface temperatures, allowing the identification and analysis of individual landscape elements. In contrast with satellite remote sensing, airborne thermal mapping allows for flexibility in prescribing the flight times. Previous research has demonstrated the capacity to relate surface temperatures to different land surface types and features, and have demonstrated that vegetation cover and urban geometries are important controls of surface temperatures.

A literature review of airborne thermal mapping for urban heat island analysis has highlighted some important themes that should be considered. Firstly, there are limitations to airborne thermal mapping, one being that it provides information on the surface urban heat island, rather than the urban canopy layer urban heat island which is most commonly referred to, and is most relevant to human thermal comfort. The airborne thermal analysis provides a bird's eye view of the surface, and hence leads to a sampling bias, as some three dimensional surfaces (e.g. walls) are neglected. The review also revealed that to make the most of airborne thermal remote sensing data, other auxiliary data can be accessed to assist in processing, analysing and interpreting the imagery. This includes aerial photography, land surface classifications, vegetation indices, LiDAR data and satellite thermal remote sensing products. Ground validation for verification of airborne thermal imagery is strongly recommended. Also, ground based air-temperature observations, through mobile transects, are routinely conducted to complement airborne thermal remote sensing, to both observe correlations between surface and air temperatures (or lack thereof), and to further understand the role of surface features in urban heat island development. Finally, it is critical that all details of the thermal capture are known to ensure accuracy in data processing.

Probably of most importance in using airborne thermal remote sensing for urban heat island analysis is an appreciation of what the data truly provides, and care is needed in interpretation given the special and specific nature of the data, as well as an appreciation of scales and surface processes influencing urban climates.

2. Methodology

The focus of this study was on the capture and utilisation of high resolution, airborne thermal remote sensing as a tool for urban planning and policy development in response to excess urban heating. A review of airborne thermal remote sensing studies presented in the Technical Report led to the development of a multi-scale, multi-technique approach to the study. This approach is represented in the flow path in Figure 1. To maximise the value of airborne thermal remote sensing data, it was recommended that a range of auxiliary data should also be acquired to assist in analysis of the thermal imagery. For detailed information on the development of this methodology, please consult the Technical Report.

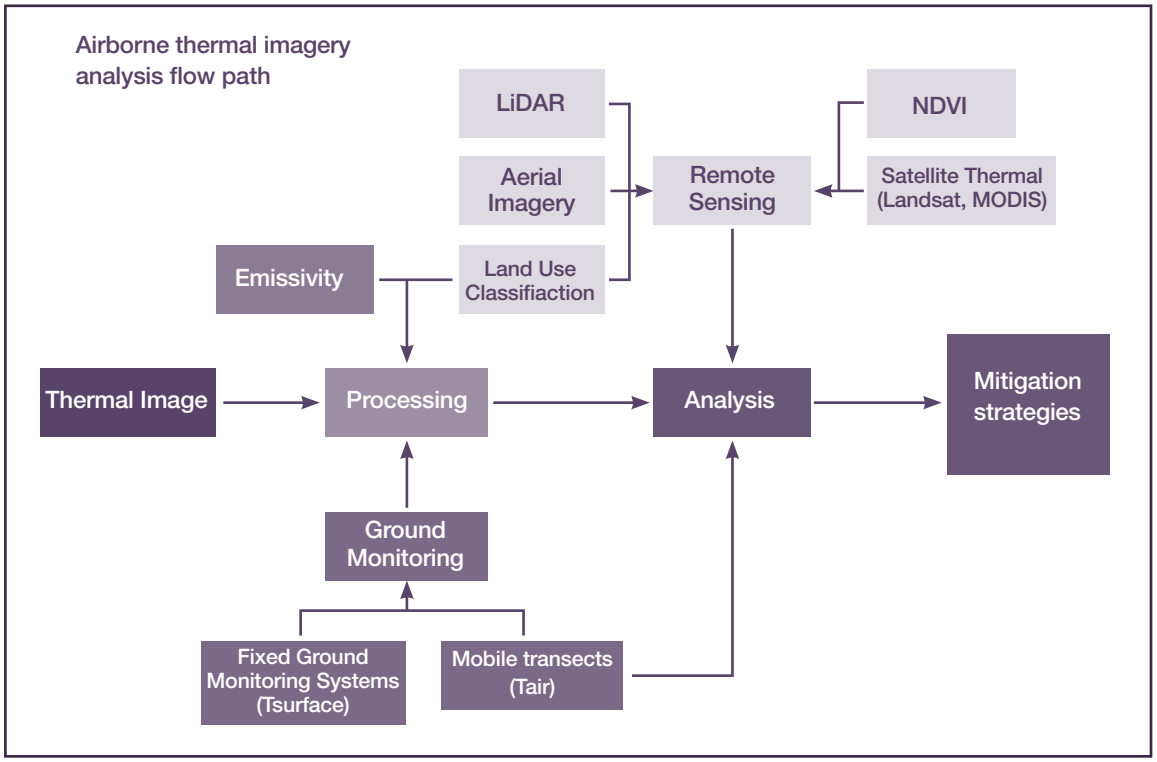

Figure 1: Overall workflow of the project and identification of auxiliary data sources for use in analysis of airborne thermal remote sensing data.

2.1 Airborne thermal remote sensing

Two local councils, the City of Melbourne (CoM) and the City of Port Phillip (CoPP) sought to undertake airborne thermal remote sensing for their municipalities during the summer of 2011-12. The location of the local council areas is presented in Figure 2. The collaborative VCCCAR project resulted in a mostly successful acquisition of thermal data, and these data were provided to the research institutions as part of the council's contribution to the project. The aim was to capture thermal imagery of surface temperatures during a period of extreme heat, so as to identify areas susceptible to intense surface warming and heat retention associated with the formation of the UHI.

Given the interest in the UHI, flights initially targeted night time conditions. The canopy layer UHI is most pronounced during the night, as urban materials absorb heat during the day and then slowly release this during the night, keeping urban areas warm relative to surrounding rural areas. The review identified that the most common time for urban thermal capture was pre-dawn, ideally between 3 am and 5 am, but flights at midnight for instance are still extremely useful, and may be more practical for data collection. The review also highlighted that the surface UHI is commonly greatest during the day as observed from satellite remote sensing (Roth et al., 1989). Daytime flights should be undertaken around solar noon to capture the point of maximum urban surface warming, and to minimise shading effects.

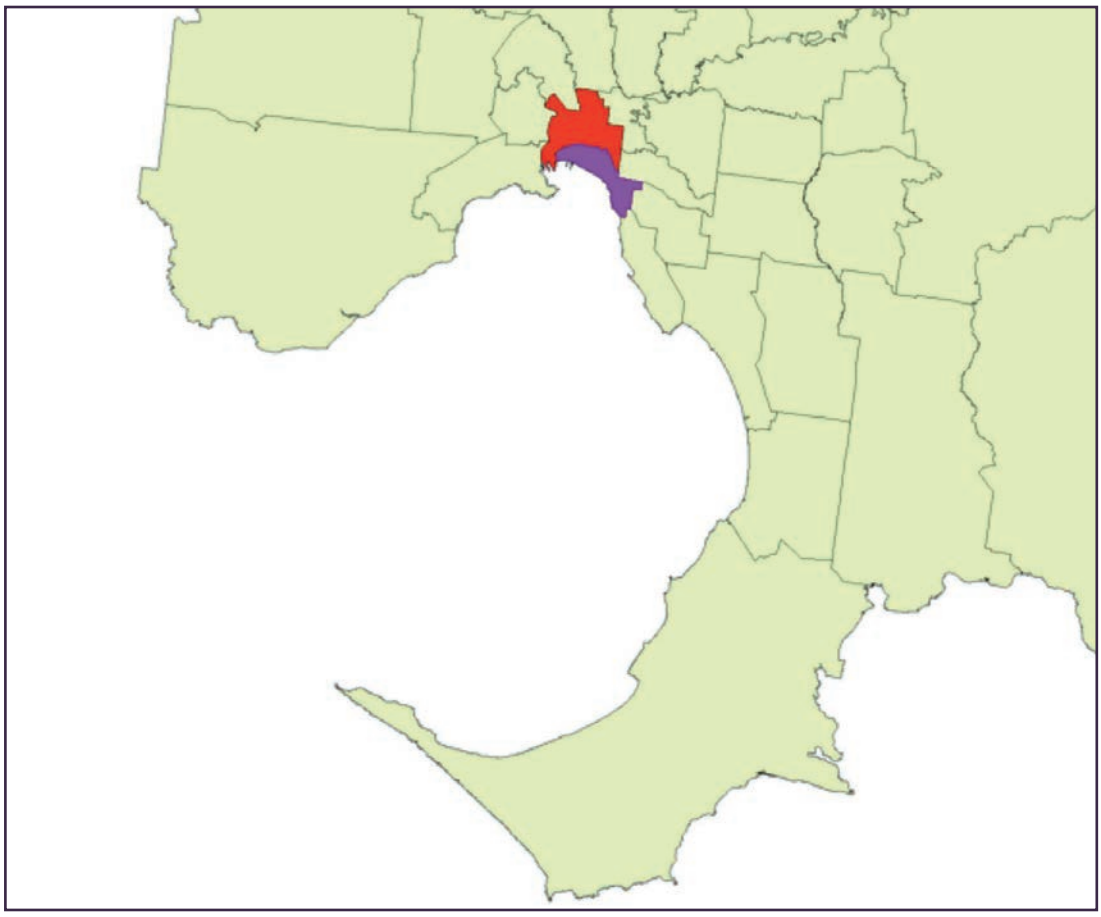

Figure 2: Local council areas mapped using high resolution airborne thermal remote sensing (City of Melbourne is red, City of Port Phillip is purple).

Once again, it is important to note that actual surface temperatures are not recorded by airborne and satellite sensors – instead Planck's law is used (the electromagnetic radiation that is emitted from a black body at an absolute temperature) to create surface brightness temperatures (Weng, 2009; Weng et al., 2004; Streutker, 2002; Streutker, 2003; Dousset and Gourmelon, 2003).

City of Melbourne

The CoM undertook a single flight between 10.45pm and 2.15am (EDT) on 24 –25 February 2012. The flight was captured using a FLIR thermal camera (FLIR is joined with Cedip Infrared Systems). The resolution of the final thermal image was 0.75 m. Images of surface radiometric temperature were compiled and then geo-referenced and mosaicked to form a single image. Some issues arose in the capture of the CoM thermal imagery, and are outlined in Appendix A. The data produced was a map of digital numbers which varied relative to changes in land surface temperature. These digital numbers were then assigned a surface temperature based on ground-based control points (discussed below) undertaken by Monash University during the flight.

City of Port Phillip

The CoPP undertook a daytime flight at around solar noon (1pm – 3pm EDT) on 25 February 2012, and a night time flight on the following night (12am – 2am EDT). The thermal data for the CoPP was also captured using a FLIR camera. The resolution of the final thermal image was 1 m. The flight was done methodically starting from the North East of the municipality and working down to the coast. Again, images of surface radiometric temperature were compiled and then geo-referenced and mosaicked to form a single image. The different image strips all overlap so that there are no areas of missing data.

2.2 Meteorological conditions

The airborne thermal remote sensing flights were undertaken during an Extreme Heat Event (EHE) from 24–26 February 2012. Using daily maximum and minimum data for Melbourne from 1979 to 2001, Nicholls et al., (2008) analysed relationships between temperature and daily mortality in Melbourne in people over 64 years of age. They found that when average daily temperatures (the mean of yesterday's maximum and this morning's minimum temperature) exceeded 30°C, there was a 15–17 per cent increase in daily mortality rates in over 64 year olds (Nicholls et al., 2008). Also, when minimum temperatures were over 24°C, there was a 19–21 per cent increase in mortality rates in over 64 year olds (Nicholls et al., 2008). Both of these threshold temperatures were reached twice during the 24–26 February 2012 observational period, indicating that the airborne thermal remote sensing data was representative of an EHE.

The air temperatures during the observational period are presented in Figure 3 (from the Bureau of Meteorology Melbourne Regional Office in the Melbourne CBD) along with the flight times of the airborne thermal remote sensing. The Technical Report identified that ideally, 2–3 sequential days of warm-hot sunny conditions would be optimal for thermal data capture, and it was critical that conditions delivered clear skies and sunny conditions. Maximum air temperatures reached 35.9°C and 36.3°C on 24 and 25 February respectively, while minimum air temperatures did not fall below 24°C on the nights of thermal data capture. The synoptic conditions at this time were typical of those that result in EHE, and are also optimal for intense UHI development at night (Morris and Simmonds, 2000), with a high pressure system positioned over the east of Victoria and the Tasman Sea, producing northerly wind flow, which brings warm, dry continental air to Victoria and Melbourne (Figure 4). Skies were clear on 24 and 25 February, before cloud appeared on the morning of 26 February, and wind speeds were generally low, particularly for the night time flights.

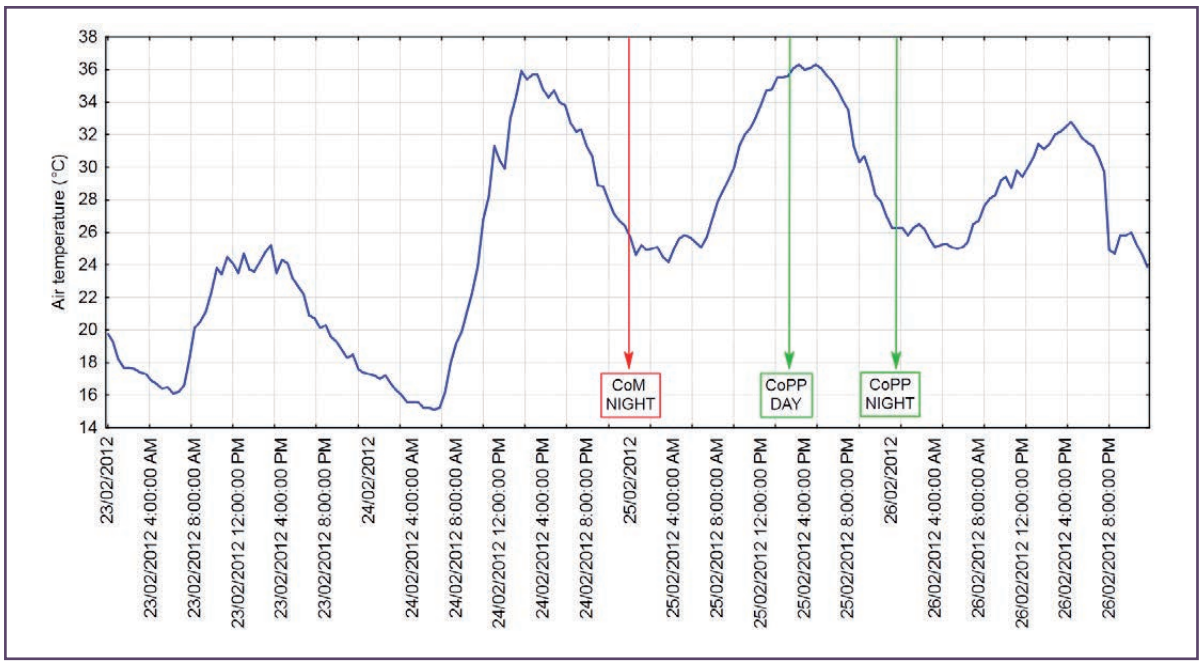

Figure 3: Air temperature during the observational period (23–26 February 2012) for the airborne thermal remote sensing, along with the corresponding flight times for each local council (CoM – City of Melbourne, CoPP – City of Port Phillip).

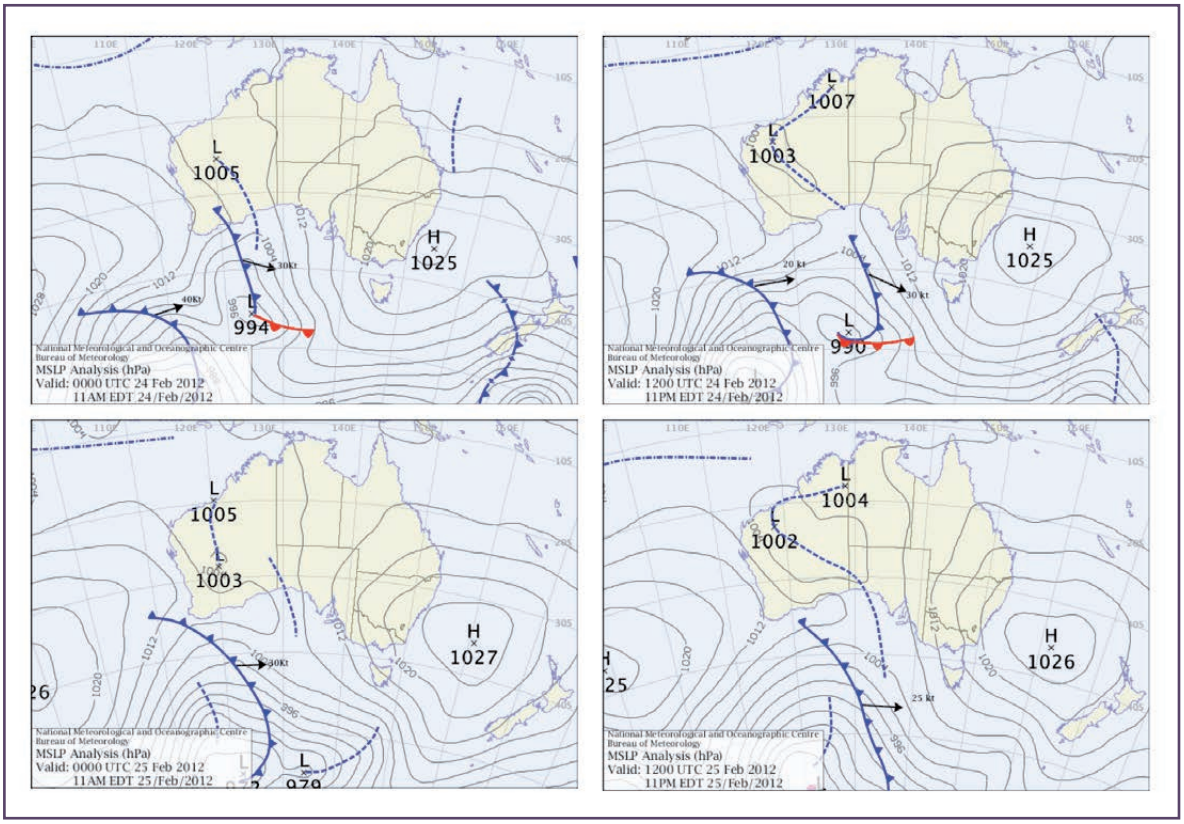

Figure 4: The synoptic situation at the time of the thermal remote sensing flights from 11am EDT 24 February 2012 through to 11pm EDT 25 February 2012 (Source: Bureau of Meteorology).

2.3 Ground based monitoring and validation of imagery

This work involved the collection of ground-based surface temperature data at fixed locations. These data allowed for an assessment of the quality of the airborne thermal imagery for data accuracy checks. A total of ten fixed ground based stations were established in early summer 2011–2012; five each within the CoM and the CoPP. These stations were established across different surface types in order to capture a range of surface temperatures. The aim was to establish these sites over large, homogeneous surfaces, so as to ensure a consistent surface temperature for comparison with the surface temperatures observed via the airborne thermal remote sensing. Establishing fixed stations meant that ground monitoring could occur regardless of the date and time of flights and did not require human resources to be in the field for this purpose. In addition to the ten fixed stations, two temporary stations were also deployed at the time of the night time flights, giving a total of 14 ground based stations over two council areas.

Ground monitoring stations comprised of a datalogger (CR1000 – Campbell Scientific) powered by a battery and a solar panel, a temperature and relative humidity probe (HMP45C – Campbell Scientific) and an infrared temperature sensor (SI-121 – Apogee). Ground validation stations were established over the following surface types: asphalt, concrete, grass, irrigated grass, galvanised steel, gravel, water and soil. Figure 5 presents photographs of some of the ground based monitoring sites. Data were recorded every 30 seconds, and block-averaged into five minute intervals.

Figure 5: Examples of the ground monitoring sites. Irrigated grass in the Melbourne Royal Botanic Gardens (left) and a rooftop at the University of Melbourne Parkville campus (right).

Table 1 presents the comparison of the surface temperature data collected at each of the ground based sites compared with the same point observed through airborne thermal remote sensing for the CoPP. As the flight time for the capture of the thermal imagery took approximately two hours for the CoPP, the flight path was accessed to determine exactly the time when the plane passed over the ground validation points to select the corresponding surface temperature. A circle of 2 m radius was used to represent the field of view of the surface temperature sensor for the ground monitoring sites.

Table 1: Comparison of raw surface radiometric temperatures from the ground based monitoring stations and the surface temperatures from the corresponding points from the thermal image for the CoPP on 25-26 February 2012.

	Night time				Daytime			
	Overpass time	Ground site (°C)	Camera (°C)	Camera st.dev.	Overpass time	Ground site (°C)	Camera (°C)	Camera st.dev.
Non-irr. grass	01:44:13	*14.83*	*17.71*	0.31	13:38:02	*60.1*	*55.06*	3.79
Gravel	01:31:49	*22.27*	*23.61*	0.18	13:20:46	*48.05*	*43.67*	2.81
Galv. Steel roof	01:39:03	*-9.46*	*-5.06*	4.20	13:32:04	*10.44*	*13.13*	0.35
Concrete	00:53:41	*27.85*	*26.97*	0.11	12:45:45	*46.1*	*43.35*	2.37
Clay	01:48:20	*19.48*	*18.82*	0.80	13:48:31	*25.98*	*42.86*	4.08
Asphalt	01:49:11	*24.78*	*22.73*	1.25				
Non-irr. grass	01:49:11	*16.54*	*19.41*	0.15				

For the comparison between the ground based data and the thermal camera data, the night time data is likely to provide a more representative comparison. During the day, greater turbulence and mixing is likely to influence the surface layer, and thermal anistrophy (directional variations in surface irradiance) will lead to differences in observed surface temperatures between each approach. Strong surface heating during the day will also generate larger temperature differences between pixels in the thermal image. As such, the night time data should be used when these effects are reduced, although the daytime is presented for interest. Generally, the agreement between the two methods was reasonable, and gave us confidence in the quality of the thermal image. Small discrepancies between the night time surface temperatures between the two methods could be a result of inaccurate representation of the field of view of the ground based sensors on the thermal image.

Unfortunately, there were some data capture issues concerning the CoM airborne thermal remote sensing. The final product supplied to the research project for the CoM area provided only a digital number that represented the surface, rather than an actual land surface temperature. Fortunately, having the ground-based stations operating, meant we could attribute surface temperatures to these digital numbers, and produce a map of surface temperature for the CoM. However, this does not allow for an assessment of the accuracy of the thermal image acquired by the thermal camera used by providers of the CoM image. More detailed information on the process of assigning values to the CoM image can be found in Appendix A.

These two situations whereby the ground-based monitoring stations were used to validate the CoPP image and to assign temperature values to the CoM image demonstrate the value in having ground-based monitoring sites. Another benefit is that the fixed ground monitoring stations complement the airborne thermal remote sensing which, while providing excellent spatial coverage, only provides one or two snapshots in time of the land surface. The fixed stations provide an excellent measure of the temporal variability in surface temperature. Data from the fixed stations are presented later in the report. An additional four sites were also established at Monash University to provide more sites for validation if required.

2.4 MODIS satellite data

Thermal imagery

MODIS (Moderate Resolution Imaging Spectroradiometer) is located on two different satellites, Terra and Aqua which are both part of NASA's Earth Observing System. Between these two satellites, the whole Earth surface is imaged every one to two days. The satellites are designed so that one crosses the equator during the morning and the other in the afternoon. This means that, depending on meteorological conditions, an image can be captured for both night and day over Melbourne. The two satellites take images in 36 bands. A number of these bands are used for thermal imaging. NASA offers Land Surface Temperature and emissivity products from these bands. These products can be gathered as a monthly average, an eight day composite and a daily image. The thermal bands provide data at 1km resolution. We used the MODIS thermal imagery to set the context for the higher resolution airborne thermal remote sensing.

For this project MODIS data were accessed from the NASA website for 24–25 of February 2012 as well as night images for both days. Corresponding to the CoM flight, the satellite MODIS image was collected at 12.20am Friday 24 February 2012 and 2.55am Saturday 25 February 2012. Corresponding to the CoPP flight, the MODIS image was collected at 3.40pm Saturday 25 February 2012 and 1.05am Sunday 26 February 2012. All the images showed a full extend with little missing data within the images, except the early morning of 26 February 2012 where some pixels were missing due to cloud cover. There was no emissivity correction applied, but the product did contain bands 31 and 32 emissivities which rely on a pixel's land cover type as determined by land cover inputs. The data product is designed to be ready for use in science applications.

Normalised Difference Vegetation Index (NDVI)

Along with thermal images MODIS also offers vegetation indices. One of the most common vegetation indices is the Normalised Difference Vegetation Index (NDVI). NDVI is calculated by using the ratio of the Red colour band and the Near Infrared band (NIR) in the equation, NDVI = NIR-RED/NIR + RED. The NDVI shows the scale of healthy vegetation in an area. The image is available on a 16–day cycle and at various different spatial scales. The image used in this project is a 16–day NDVI composite with a 1km resolution from February 2012.

2.5 LiDAR

Light Direction and Ranging (LiDAR) data is collected by sending pulses of light at the target and recording the return signal to calculate distance. LiDAR normally uses visible, ultraviolet and infrared wavelengths. LiDAR provides high resolution information on building heights which allows for the estimation of a range of urban morphological parameters. In this study, building heights were used to calculate street canyon Height to Width ratios (H:W). LiDAR has previously been collected for the greater Melbourne area and LiDAR building heights were obtained from both CoPP and CoM.

2.6 Air temperature transects

While the focus in this study is land surface temperature, the broader interest in excess urban temperatures identifies more with the canopy layer air temperatures: the air temperatures experienced by pedestrians. Our review highlighted that some studies showed good correlations between surface and air temperature (Saaroni et al., 2000), while others did not (Eliasson, 1992). Surface to air temperature correlations are strong under more stable atmospheric conditions, but surface to air temperature relations become decoupled under higher wind velocities (Stoll and Brazel, 1992) and correlations between surface and air temperatures improve at night, when micro-scale advection is reduced (Unger et al., 2010).

To observe surface and air temperature relationships, we conducted a number of air temperature transects at the time of the night time airborne thermal image capture. This was done using a datalogger (CR1000 – Campbell Scientific) and a temperature and relative humidity sensor (HMP45C – Campbell Scientific). An East-West transect across Melbourne was completed during each of the night time thermal flights (Figure 6). This aimed to provide an indication of the intensity of the canopy layer UHI (urban-rural temperature contrast) at the time of the flights compared with the MODIS thermal imagery. In addition, transects were also conducted within each of the local council areas (Figure 6) to document intra-council temperature variation and compare temperature patterns with the surface temperatures captured via the airborne thermal remote sensing.

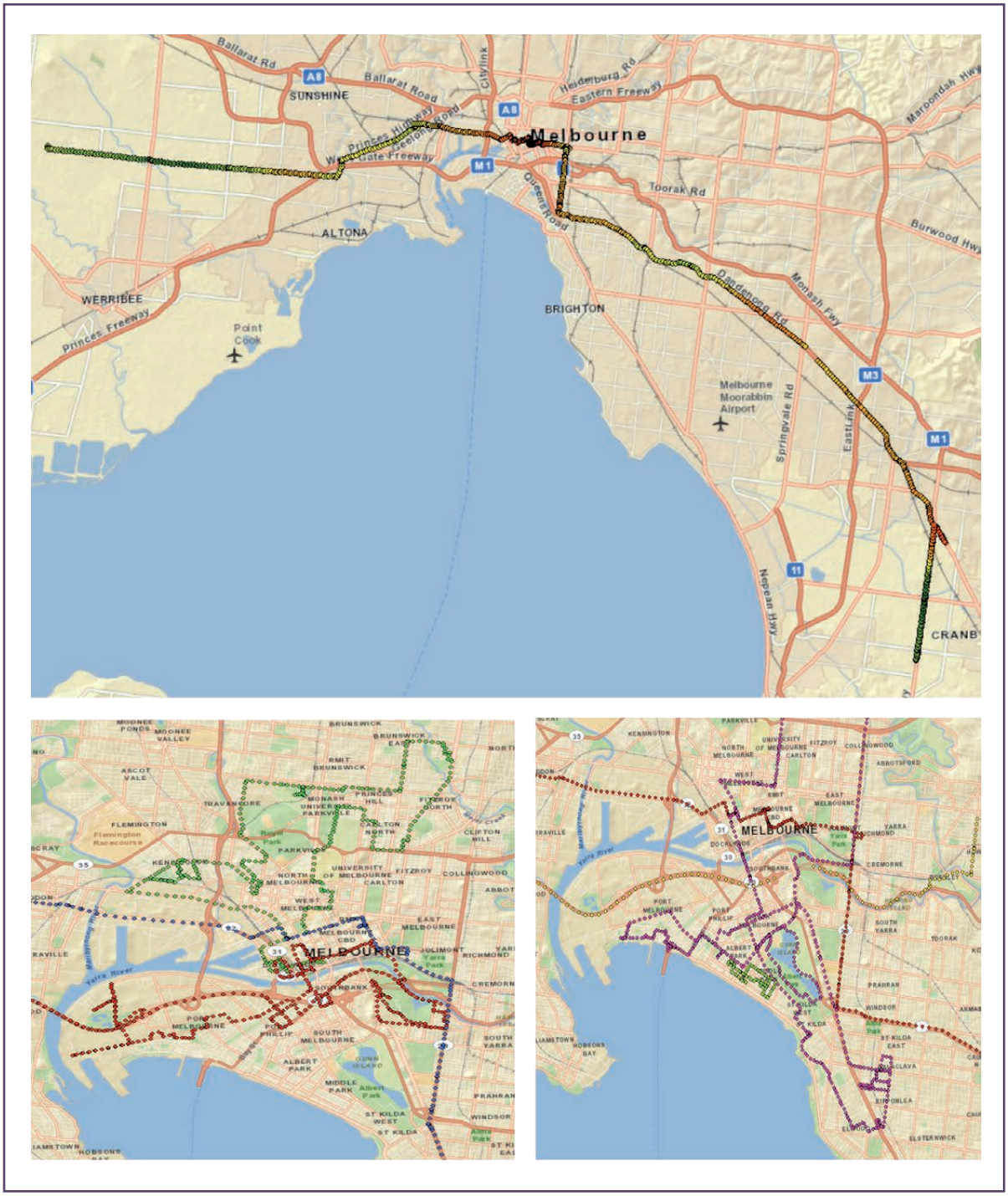

Figure 6: Map of air temperature transects conducted during the airborne thermal remote sensing flights. The East-West transect was conducted 24–25 February 2012 (upper panel), CoM transects on 24 February 2012 (lower left) and CoPP transects on 24 February 2012 (lower right).

2.7 Land surface classification

Land surface classifications assist in the analysis and interpretation of the airborne thermal remote sensing data. Using aerial imagery or other remote sensing products such as multi-spectral data or hyper-spectral data, the land surface can be classified into a number of dominant surface classes. Most classifications commonly define seven classes: buildings, roads, trees, grass, concrete, bare ground and water. Multi-spectral and hyper-spectral data is more useful for land surface classifications as these products have more

wavelengths (rather than just red, green and blue seen in an aerial image) with which to train the supervised classification algorithms in GIS software and distinguish different surface types. Nine classes were defined for this study which included the seven listed above, but with grass separated into irrigated and non-irrigated, and buildings separated into tiled roofs and galvanised steel roofs.

Selection of focus areas

Two focus areas were selected within CoPP for more detailed analysis (Figure 7). Sites were selected based on providing a comparison of different land use characteristics, along with future policy intentions in consultation with the local government research partners. Also, by selecting focus areas, the supervised classification of the surface could be adjusted manually to improve the classification accuracy. Focus areas were sized according to the area that might be a focus for implementation of green infrastructure, such as in a precinct plan.

1. *Middle Park – City of Port Phillip:* This area was selected as it is a highly vegetated low density neighbourhood allowing for a focus on the effect of green space on surface temperature.

2. *South Melbourne – City of Port Phillip:* This area was selected as a high density area with little vegetation cover. This area was also selected because it was identified as a priority area for redevelopment and could be a site for future greening interventions.

Figure 7: Selected focus area with the manually edited, supervised classification for Middle Park (left) and South Melbourne (right).

City of Port Phillip

The CoPP had remotely sensed multi-spectral data available, captured on 5 April 2012, for their municipality with which to complete the land surface classification. The focus areas were selected to complete a manual, edited, supervised classification to ensure accurate representation of the surface (Figure 8). In addition to the focus areas, we also attempted to classify the entire CoPP area using a supervised classification. The land surface classification also attempted to separate out the buildings into galvanised steel roof and tiles roofs using the multi-spectral image. The raw thermal image was also used to help determine the land surface type, particularly with regard to the rooftops. Using both the multi-spectral image and the raw thermal image provided more bands of the electromagnetic spectrum to help define the land surface. Given the size of the entire municipality, it was simply not feasible to undertake a manual correction of the classification, and errors evolve as a result of incorrectly classified pixels. This became an issue when using the land surface classification for correcting the thermal image for emissivity (discussed later). Another issue is the presence of shadows. If the aerial or multi-spectral image is not collected close to solar noon in summer, then shadowing becomes an issue. A supervised classification will struggle to determine what the surface type is where a shadow is cast and will influence the results if analysing land surface and surface temperature relationships. As such, an additional class for shadows was added. In the smaller focus areas however, the shadow areas can be manually prescribed to a class.

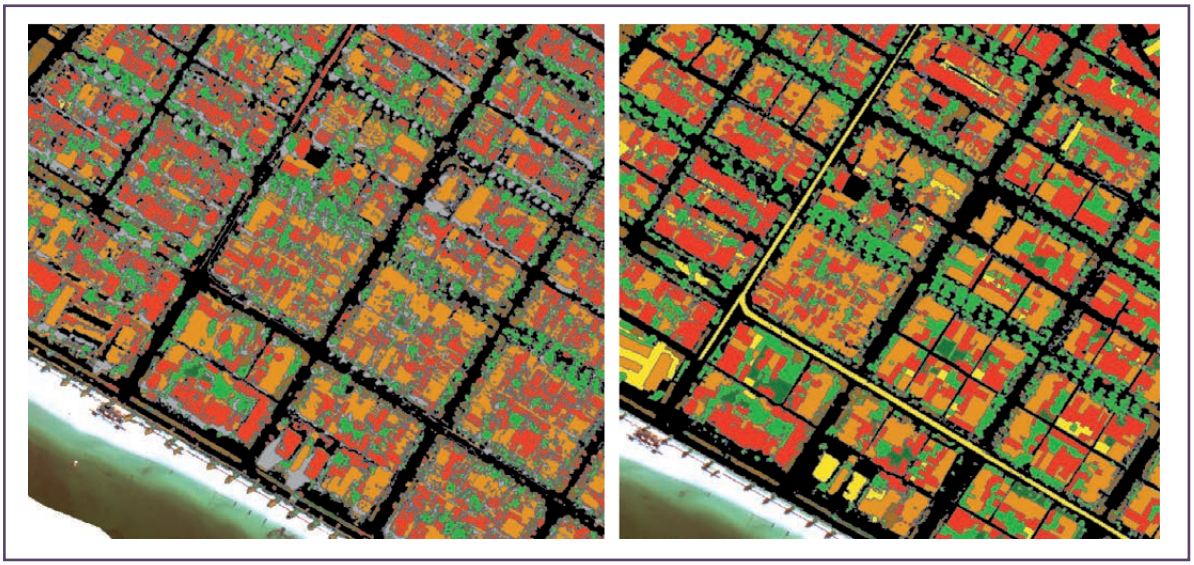

Figure 8: Land surface classification within the Middle Park focus area using an automated supervised classification in GIS software (left) and a manually edited supervised classification of the same area (right).

By comparing the supervised classification for the whole CoPP area with the more accurate focus areas, we could get an assessment of the accuracy of the supervised classification (Table 2). Assuming the manual classification was correct, the average surface temperatures for each surface type varied by up to 3.34°C as a result of the alternate classification method but were generally less than 1.5–2°C. A 500 random point accuracy assessment was done on the supervised classification compared showed an accuracy of 88.4 per cent of correctly assigned pixels based on the aerial image (Appendix B). This means that of the 500 points assessed 11.6 per cent of the surface of the entire CoPP land surface was incorrectly classified. This should be kept in mind when the analysis is conducted on the entire CoPP image. This comparison neglects the areas of shadow in the supervised classification, where the surface type cannot be identified. The contrast between the two methods is clear in Figure 8 with the manual classification using visual methods for identification appearing more accurate. The effects of the shadows in the supervised classification are also clear in Figure 8.

Table 2: Mean surface temperature differences between the supervised classification of the entire CoPP and the manually edited supervised classification of the focus areas for each land cover type. The thermal images were corrected for emissivity.

	South Melbourne		Middle Park	
Surface	DAY	NIGHT	DAY	NIGHT
Concrete	2.23	2.24	0.95	0.87
Irrigated Grass	1.05	0.57	1.79	1.88
Non Irrigated Grass	1.29	0.77	0.85	0.63
Road	0.23	0.30	-0.04	0.05
Tile Roof	-1.22	-0.90	-0.86	-0.83
Tin Roof	-1.39	-1.28	-1.81	-1.76
Trees	0.93	0.37	0.72	0.71
Water	0.19	1.05	2.98	3.34

2.8 Emissivity corrections

Remote sensing of a surface through an infrared thermal camera or an infrared temperature sensor actually measures surface irradiance, that is, longwave radiant energy leaving a surface in W/m^2. Surface irradiance is directly related to the temperature of the surface governed by the Stefan-Boltzman equation which is:

$$\textbf{Energy emitted} = \sigma \varepsilon T^4$$

where Energy Emitted is in W/m^2, σ is the Stefan Boltzman constant (5.67×10^{-8}), ε is the surface emissivity, and T is the temperature in degrees Kelvin. Emissivity is the ability for a surface at a given temperature to emit radiation, and ranges from 0 to 1.

When a thermal image is collected and converted to a surface temperature, emissivity is often assumed to be 1 or a representative emissivity (such as 0.95 for urban areas) is applied to the entire image. This approach may be suitable for coarse scale thermal remote sensing (e.g. MODIS), but for high resolution airborne thermal imagery, individual surfaces like roads, buildings and trees become clear and should be treated separately. Airborne thermal remote sensing tends to underestimate the actual surface temperature as a result. The lower the emissivity, the larger the error in surface temperature observation if left uncorrected. Also, surfaces reflect longwave radiation (from the sky) which is also observed by the sensor or camera and can also be corrected for, if longwave radiation from the sky is measured. This effect tends to be small for surfaces with a high emissivity, but for surfaces with low emissivity, longwave reflectance can be high, and should also be corrected for.

In this study, we use the land surface classification described above to define each surface type, and then apply a single value for emissivity for each surface type. Values for emissivity drawn from the literature are presented in Table 3. Emissivity values can tend to vary in the literature, so values were chosen that were most representative of those reported from the variety of literature sources drawn on. What were deemed to be reliable sources, and sources that were cited by others were used. Reflected longwave radiation was not corrected for, as longwave radiation from the sky was not measured.

Roofs saw the largest variability in documented emissivity values. Depending on the roof type, emissivity values could range anywhere between 0.25 to 0.9 and also depended on factors like how weathered a surface was. From the land classification using only multispectral data or aerial imagery, it was difficult to distinguish different roof surface types. We attempted to separate rooftops into two classes of tile roofs and galvanised steel roofs based on the multi-spectral image and the thermal signature, but it was not possible to break this down any further. So, while an emissivity of 0.86 was applied to galvanised steel roofs, some of these roofs would have emissivity as low as 0.25, so the surface temperature presented in the spatial maps will be significantly incorrect.

Table 3: Selected values of emissivity for different surfaces as well as sources used.

Surface type	Emissivity	Source
Concrete	0.94	Oke, 1987
Water	0.97	Oke, 1987
Grass	0.98	Geiger et al. 2003
Trees	0.98	Oke, 1987
Asphalt	0.95	Oke, 1987
Tiled roofs	0.90	Oke, 1987
Galvanised steel roofs	0.86	Multiple sources
Clay	0.95	Arya, 2001
Gravel	0.92	Harman, 1994

Challenges surrounding emissivity corrections will be discussed further in the results and discussion section, but to demonstrate the range of error that could be expected from an incorrect emissivity value, Table 4 presents an example for a surface with a remotely sensed temperature of 25°C. For this example, the irradiance observed by the sensor is 448.05 W/m2 for a surface with an emissivity of 0.95. If this emissivity was not corrected for, the surface temperature would be underestimated by 3.85°C. Table 4 presents the error associated with a 0.01 change in emissivity from the correct emissivity of 0.95. This should be kept in mind when interpreting thermal imagery.

Table 4: Example of the influence of emissivity on absolute surface temperatures and associated error for incorrect application of emissivity values.

T^{surf} Observed (°C)	Irradiance (W/m^2)	Emissivity	T^{surf} Corrected (°C)	Error (°C)
25	448.05	1.00	25.00	3.85
25	448.05	0.99	25.75	3.10
25	448.05	0.98	26.51	2.34
25	448.05	0.97	27.28	1.57
25	448.05	0.96	28.06	0.79
25	448.05	0.95	28.85	0.00
25	448.05	0.94	29.65	0.80
25	448.05	0.93	30.46	1.61
25	448.05	0.92	31.28	2.43
25	448.05	0.91	32.11	3.27
25	448.05	0.90	32.96	4.11

Correcting for emissivity is probably the largest limitation in high resolution airborne thermal remote sensing. Grimmond et al., (2010) state that there have been few studies that have explicitly examined urban emissivity. Previous studies using high resolution airborne thermal remotes sensing data either neglected an emissivity correction (e.g. Saaroni et al., 2000), or used surface irradiance rather than surface temperature in analysis so correcting for emissivity was not needed (e.g. Lo et al., 1997). Given our research partners interest in surface temperature, we attempted the emissivity correction and focused on surface temperature. An additional source of error in this process surrounds the land surface classification, whereby any pixels that are incorrectly assigned to a particular class would be assigned an incorrect emissivity value. So, the accuracy of the emissivity correction is also dependent on the accuracy of the land surface classification and the quality of the data products.

2.9 Ground based thermography

An identified limitation of airborne thermal remote sensing is that it presents a biased view of the surface in that some of the 3D structures of the surface (e.g. walls) are neglected. As part of our methodology we undertook a thermography transect through a small area of the CoPP at the time of the thermal flight on 25 February 2012. This transect allowed us to view the surface temperature of walls and surfaces below tree canopies. We used a TP8 Thermopro thermal camera mounted on a car to conduct the transect. These images were used to complement the analysis.

In addition, ground-based thermography was conducted on a green façade on the Corkman Pub on 20 March 2012 on the corner of Leicester Street and Pelham Street in the City of Melbourne. The green façade is located on a north facing wall on a street that is 30 m wide with low rise buildings opposite which meant that the wall was not impacted by shadows. Thermal images were taken every five minutes between 9.15am and 5.30pm. The maximum temperature on 20 March 2012 was 27.2°C.

Ground thermography was also conducted for a living roof located on the Monash City Council, council chambers roof on 5 April 2012. The roof has different types of succulent vegetation on it and the roof is located in an area that is not surrounded by any buildings that would significantly shadow it. Thermal images were captured every five minutes between 10am and 6pm. The maximum temperature on 5 April 2012 was 26.8°C.

3. Results and discussion

The structure of the results and discussion will be presented in order of scale, moving from the city scale (meso-scale) down through to the neighbourhood (local-scale) precinct and building scale (micro-scale). Given some of the limitations concerned with the data collection for the CoM data, the CoPP data is primarily used throughout the results and discussion.

3.1 City-wide urban heating and vegetation cover

Over the Extreme Heat Event (EHE) period in late February 2012, city wide measures of land surface temperature (LST) were acquired through MODIS in order to place the data from high resolution thermal remote sensing within the broader context of urban warming. In addition, a satellite image of NDVI was collected (Figure 9) as an indication of relative variations in vegetation cover across the Melbourne metropolitan area. Figure 9 demonstrates the clear vegetation gradient across Melbourne from west to east, with the Eastern/South Eastern local council areas having a higher vegetation cover and areas of sparse vegetation occurring in the CBD and areas such as Dandenong.

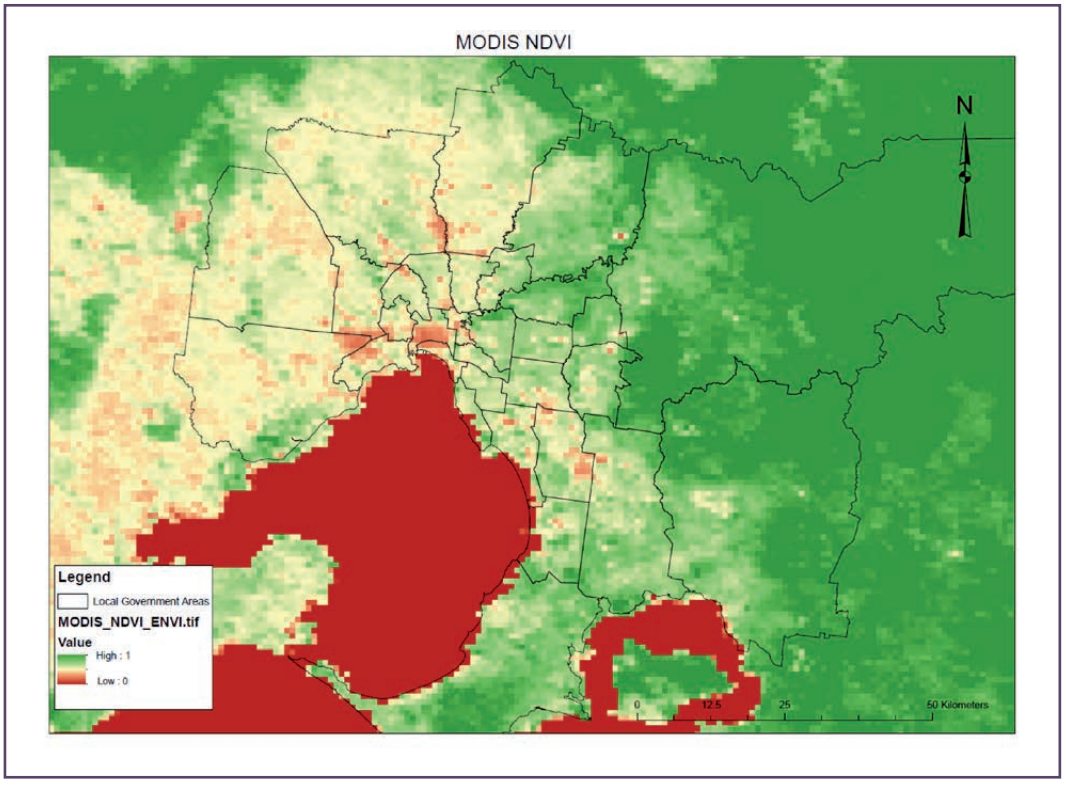

Figure 9: Normalised Difference Vegetation Index (NDVI) for the Melbourne metropolitan area in February 2012.

Figure 10 presents the daytime and night-time MODIS LST images for 24 February 2012, reflecting the conditions for the CoM night time flight. Figure 11 presents the daytime and night-time MODIS LST images for 25 February 2012, reflecting the conditions for the CoPP daytime and night time flights. Similar patterns were seen for the MODIS LST during the day, with the western local council areas of Melbourne showing LSTs as high as 50°C (City of Melton), as the dry basalt plains and grasslands heat intensely during the day. During the day, the presence of a surface UHI was evident (urban-rural LST differences).

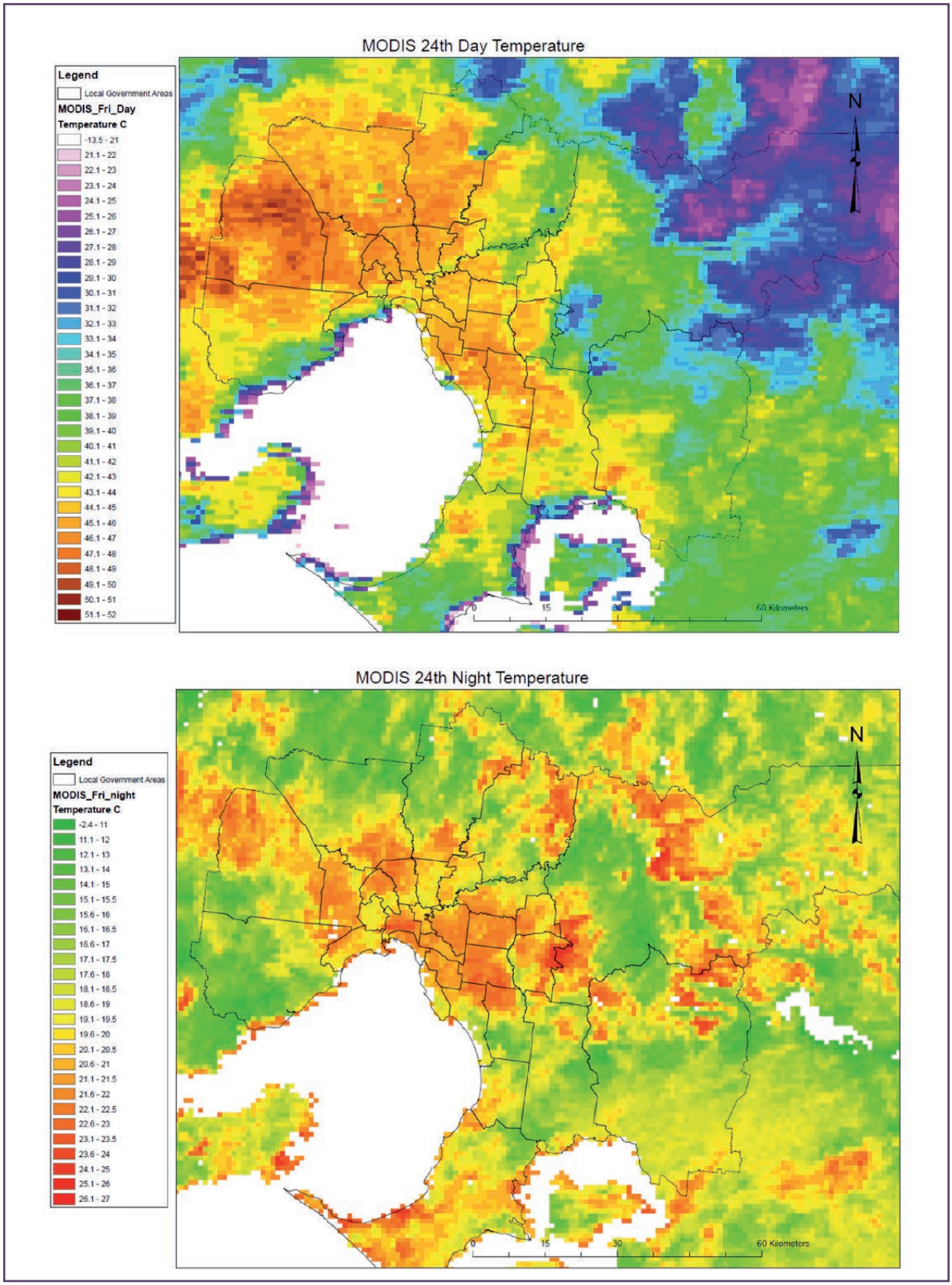

Figure 10 presents the daytime and night-time MODIS LST images for 24 February 2012, reflecting the conditions for the CoM night time flight.

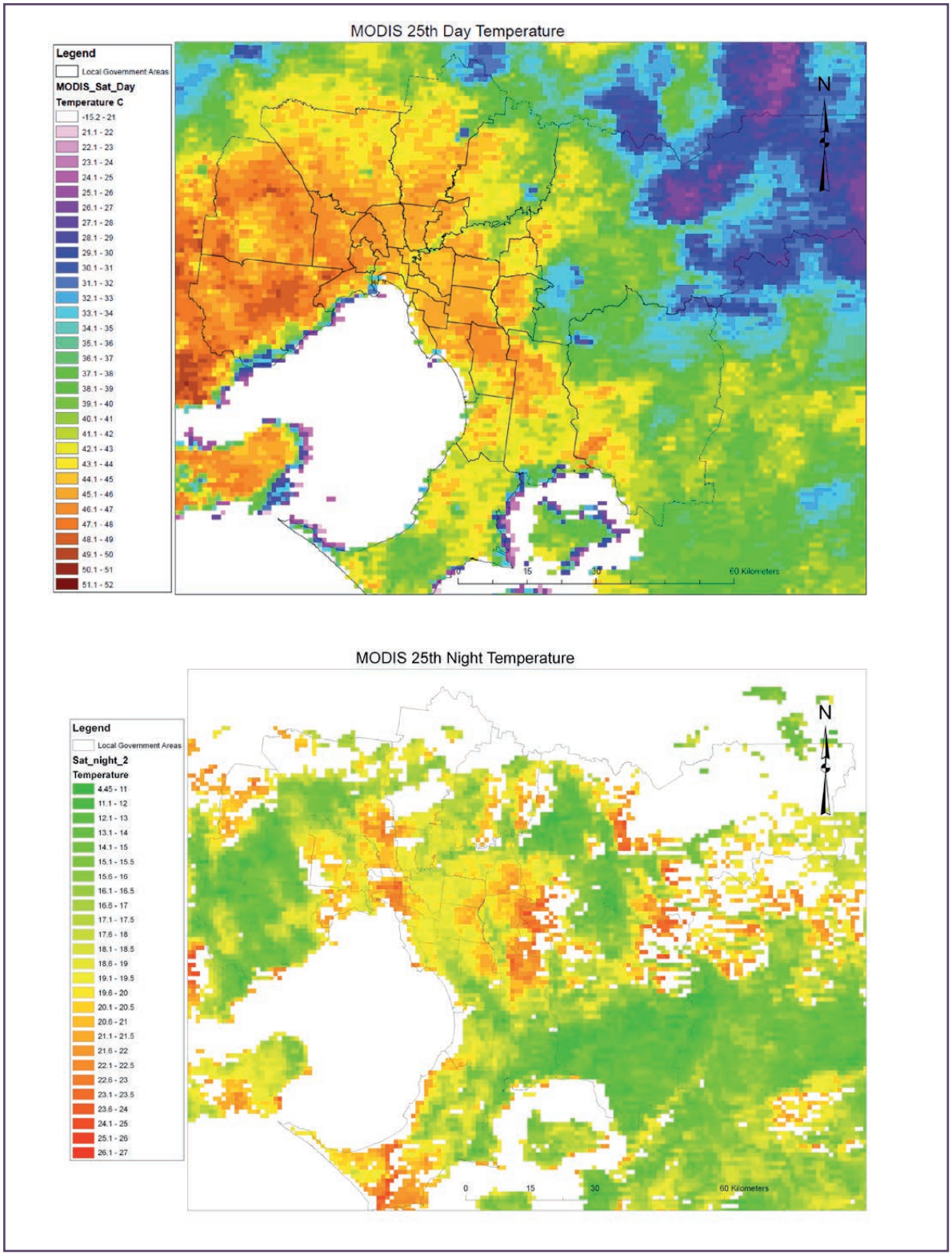

Figure 11: MODIS LST 25 February 2012: 3:40pm (upper panel) and 1:05am (lower panel) City of Port Phillip flights. White areas represent missing data. Different colour schemes are used for daytime and night-time images to maximise contrast, but the scales are the same as Figure 10 to allow comparison between days.

The intense heating during this extreme weather event resulted in widespread warming across both rural and urban landscapes, with some cooler zones evident in coastal and vegetated mountainous areas. Comparing the land surface temperatures of all the local government areas in Melbourne, maximum land surface temperatures in the CoM from the MODIS were amongst the highest during the day showing 48.1°C and 47.83°C on 24 and 25 February 2012 respectively. Maximum land surface temperatures in CoPP were amongst the coolest of the local government areas showing 43.4°C and 45.6°C on 24 and 25 February 2012 respectively.

At night, the surface UHI is clearly distinguishable and aligns more closely with the extent and density of the urban area. This was particularly apparent on 24 February 2012. The urban surfaces remain warm at night in areas such as the CBD where surface temperatures were as high as 23.5°C as a result of heat retention, while the rural areas cool rapidly. At night, the surface UHI intensity (peak in surface temperatures differences between CBD and rural areas) could reach as high as 9°C. The white patches in the lower panel of Figure 11 represent missing data due to growing cloud cover.

The MODIS LST figures demonstrate the surface UHI, and in order to achieve an understanding of the canopy layer UHI, an air temperature transect was conducted to ascertain whether patterns of land surface temperature were similar to canopy layer air temperatures. Figures 12 and 13 present a west to east transect across Melbourne (described in the methods) conducted 24–25 February 2012, corrected to 1am. NDVI is also presented. Results indicate that patterns of surface and canopy layer air temperature are very similar, and correspond relatively well with vegetation cover (NDVI). The clear 'island' shape commonly seen in UHI plots is not well pronounced yet the commonly documented 'cliffs' (rapid drops in temperature at the boundary of the city) are evident. The central city area is relatively warmer than the rural surrounds, with surface temperatures (T_{surf}) peaking at 23.5°C and air temperatures (T_{air}) peaking at 29.8°C on the night of the CoM flight. There was clear spatial variability across the length of transect, due to variations in vegetation cover, but also other UHI drivers such as total impervious cover and density of buildings. Areas with low vegetation cover tend to show high surface and canopy layer air temperatures. It is difficult to define what is exactly 'rural' in this instance, but broadly, the maximum canopy layer UHI intensity was around 6-7°C during the collection of the night time thermal imagery for CoM and CoPP.

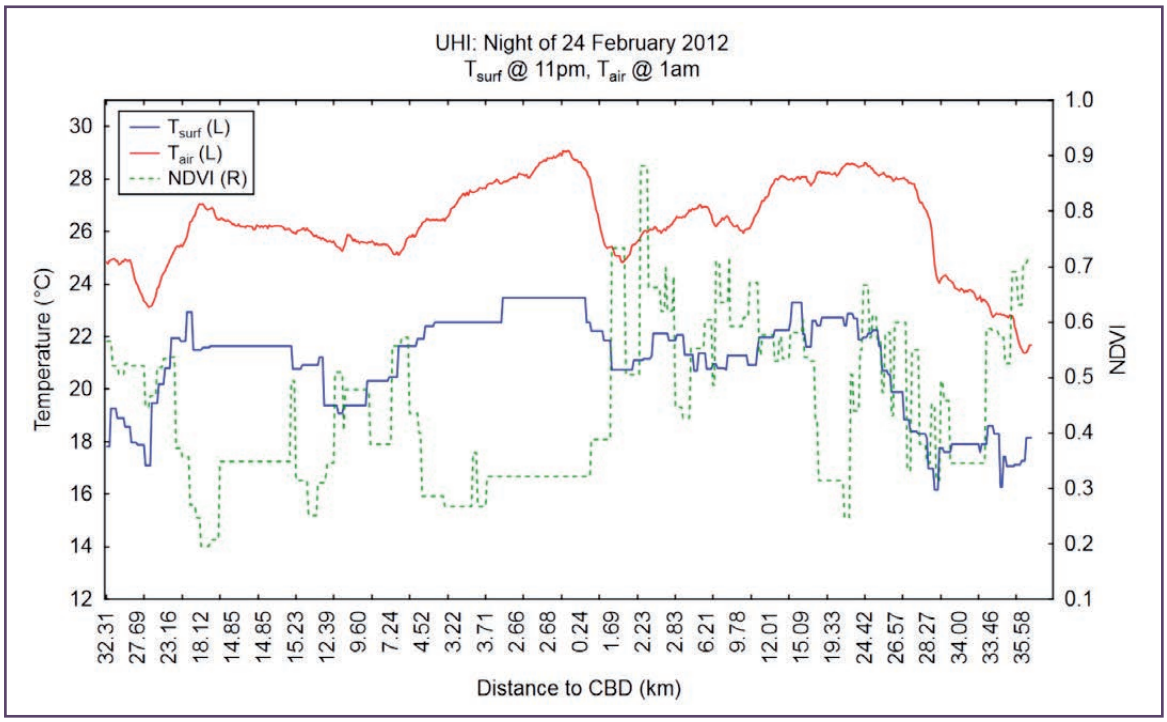

Figure 12: West-east UHI transect 24 February 2012. The air temperature transect is corrected to 1am. The MODIS surface temperature data corresponds to 2.55 am. NDVI values indicate fraction of vegetation cover. CBD was taken as 37° 48' 51.0906", 144° 57' 47.2782" (intersection of Swanson St and Bourke St, Melbourne).

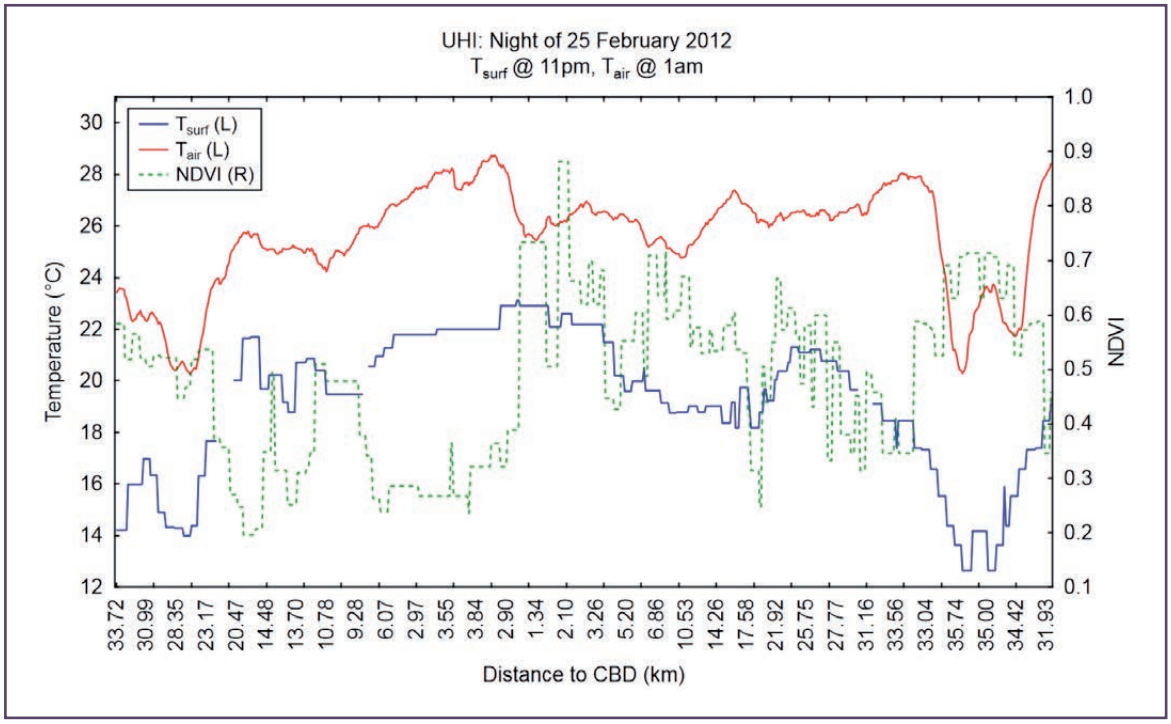

Figure 13: West-east UHI transect 25 February 2012. The air temperature transect is corrected to 1am. The MODIS surface temperature data corresponds to 1.05am. NDVI values indicate fraction of vegetation cover. CBD was taken as 37° 48' 51.0906", 144° 57' 47.2782" (intersection of Swanson St and Bourke St, Melbourne).

It should be acknowledged here that there is a mismatch in scales in Figure 10 and 11, with NDVI and MODIS LST representing the local scale (e.g. 1 km), while the air temperature measures are a micro-scale measurement (e.g. 100 m). As such, analysis of correlations between canopy layer air temperatures and land surface temperatures, along with NDVI cannot be done in a meaningful way. Nevertheless, this suggests that MODIS land surface temperature data provides a good local scale approximation of air temperature *patterns* during extreme heat events, though surface to air temperature difference will vary temporally.

This city wide analysis using freely available MODIS LST data has set the context for the finer scale analysis of the areas mapped using airborne thermal remote sensing. The airborne thermal remote sensing was undertaken at a time when the night time canopy layer UHI intensity was high.

3.2 Local scale urban heating and vegetation cover

Appendix C presents the high resolution airborne thermal remote sensing maps for the City of Melbourne on 24 February 2012 as well as the daytime and night-time images for 25 February 2012 for the City of Port Phillip. Here, example thermal maps for parts of the two focus areas are presented to provide a clearer indication of land surface temperature variations between different surface types and urban configurations (Figures 14 and 15 – note different temperature scales). The 1 m resolution of these maps allows for the identification of individual landscape elements in the thermal image, unlike data from MODIS or Landsat ETM+ where the resolution is too coarse. Figures 14 and 15 highlight that during the night, roads and other impervious surfaces were warmer than vegetated surfaces like trees and grass. Similar patterns are seen for the CoPP daytime images. Areas of high surface temperature (hot-spots) can be clearly identified. Some rooftops appear very cool relative to other surfaces. This is due to the effect of surface emissivity and the application of one value for emissivity for the land surface temperature correction of galvanised steel roofs (or similar rooftop materials) along with incorrect surface classification (classified as concrete rather than galvanised steel roof). These surfaces have a very low emissivity and as such, the surface temperature was underestimated.

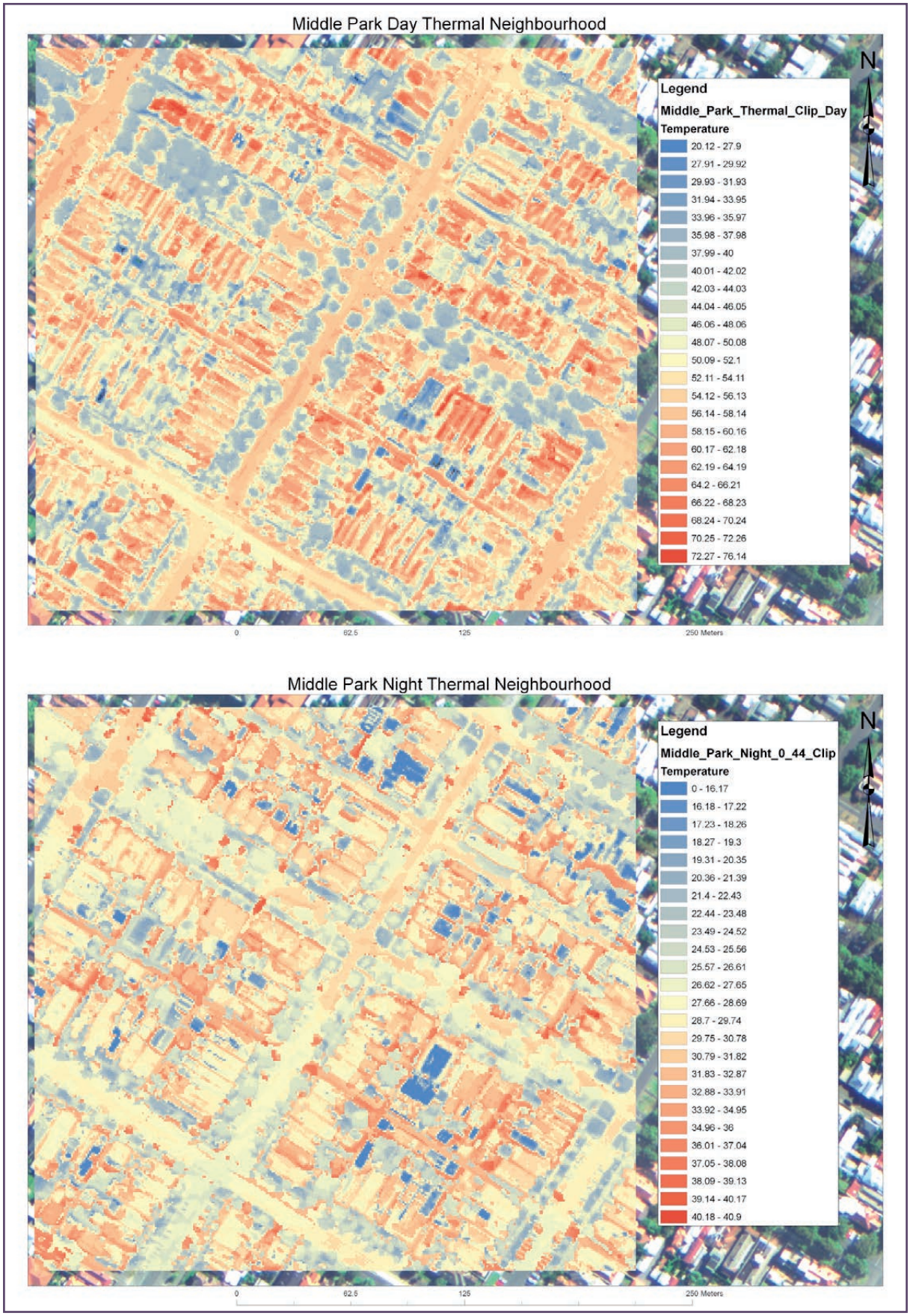

Figure 14: Example of the corrected thermal imagery for an area within the Middle Park focus area during the day (upper panel) and night (lower panel). Note different scales are used.

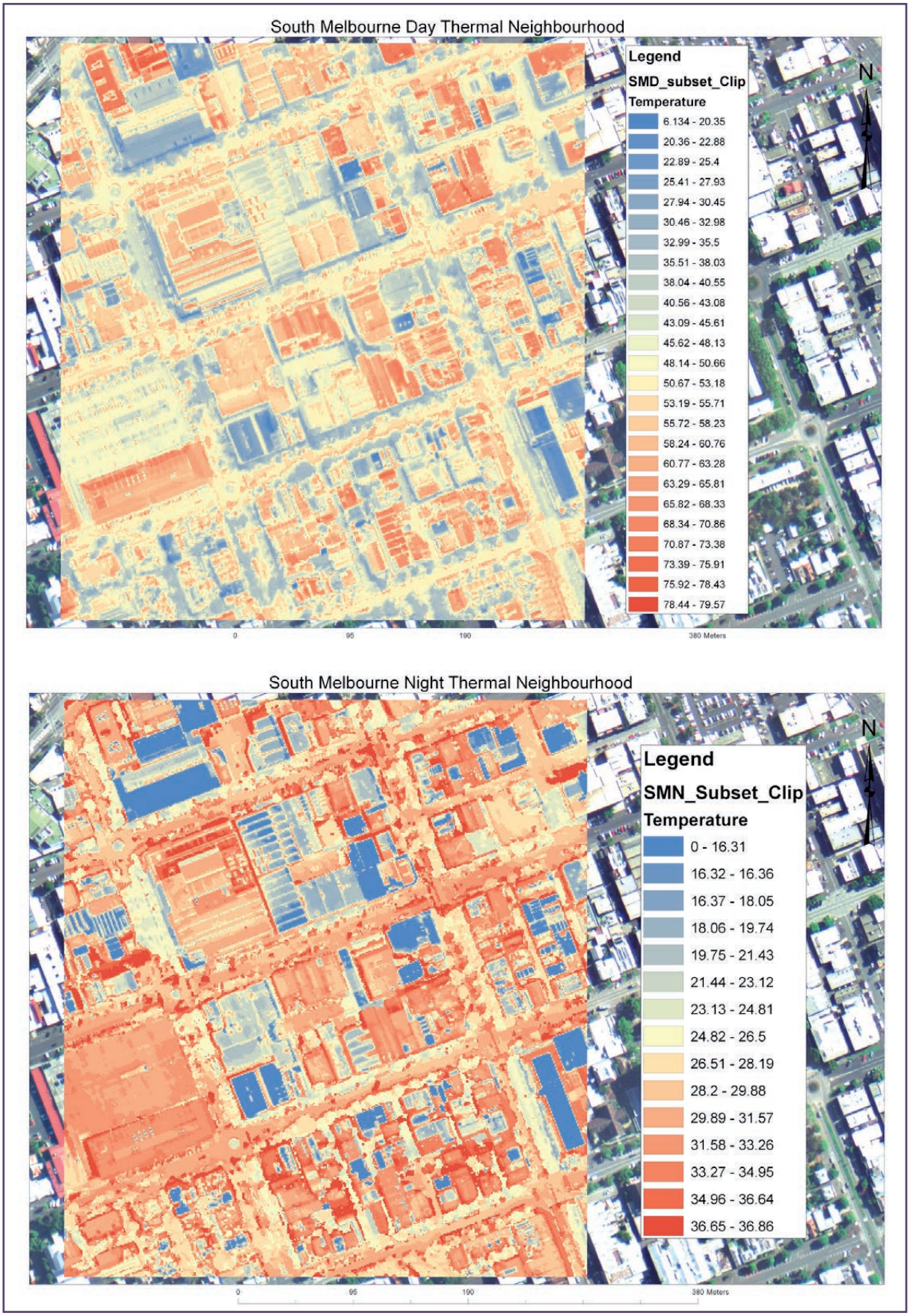

Figure 15: Example of the corrected thermal imagery for South Melbourne focus area during the day (upper panel) and night (lower panel). Please note different scales are used.

To identify the surface temperature variations between different surface types, the land surface classification was used for each focus area, and the average land surface temperatures for CoPP are presented in Table 5 for CoPP. During the day, tiled rooftops showed the highest land surface temperatures (52.20°C and 53.54°C) due to direct exposure to solar radiation where shading effects could not be felt and also due to the high heat absorption of rooftop materials, while trees showed the lowest land surface temperatures (41.59°C and 43.61°C). Irrigated grass was 3.58-5.19°C cooler than non-irrigated grass due to evaporation at the surface and dissipation of heat through moist soil (Figure 16). Similar patterns were observed at night, with roads remaining relatively warm compared to other surfaces, due to large heat storage during the day, as well as trapping of heat within urban canyons. LST differences between irrigated and non-irrigated grass become small, as non-irrigated grass cools rapidly compared to irrigated grass (Figure 16), and was the coolest surface at night in the Middle Park focus area. These data clearly identify the role that urban materials play in increasing land surface temperatures, and that capacity for increasing natural surfaces, particularly trees and irrigated grass can have in lowering land surface temperatures. The challenge is in identifying places and spaces to integrated vegetation into the urban landscape.

Table 5: Average LSTs of the major land surface types for the City of Port Phillip focus areas.

South Melbourne	DAY (°C)	St. Dev. (°C)	NIGHT (°C)	St. Dev. (°C)
Concrete	50.45	7.66	31.63	5.26
Irrigated grass	42.81	8.34	25.59	3.92
Non irrigated grass	48.00	6.80	26.27	3.74
Road	48.83	7.63	29.16	4.28
Tile roof	52.20	7.82	30.35	4.35
Galv. steel roof	51.95	11.20	26.53	8.60
Trees	41.59	6.66	26.62	2.90
Water	44.41	7.97	27.72	3.90
AVERAGE	**47.53**		**27.98**	
Middle Park	**DAY (°C)**	**St. Dev. (°C)**	**NIGHT (°C)**	**St. Dev. (°C)**
Concrete	50.22	7.61	28.69	4.97
Irrigated grass	45.56	7.75	26.04	4.57
Non irrigated grass	49.14	6.54	24.94	3.14
Road	51.14	7.00	28.20	3.46
Tile roof	53.54	7.18	28.69	3.90
Tin roof	52.95	9.01	28.38	6.89
Trees	43.61	6.56	26.03	3.19
Water	48.02	6.71	29.42	5.04
AVERAGE	**49.27**		**27.55**	

Standard deviations in LSTs provided in Tables 5 indicate that there is a wide amount of variability within each surface type. Variability is particularly large for galvanised steel roofs, again highlighting the issues around emissivity correction using one value. Also, some of this variability will be due to misrepresented pixels in the land surface classification.

Another point to note here is that the LSTs are much higher than the land surface temperatures observed from the MODIS satellite images presented earlier. Average night-time temperatures from the airborne thermal remote sensing data were around 27.5–28°C, while the maximum LSTs observed via MODIS across the CoM and CoPP areas were 2–3°C cooler. The coarse resolution of the MODIS imagery washes out the variability across the landscape, and methodological approaches to processing MODIS imagery may lead to an underestimation of the surface temperatures. Differences may also arise from differences in approaches for emissivity corrections.

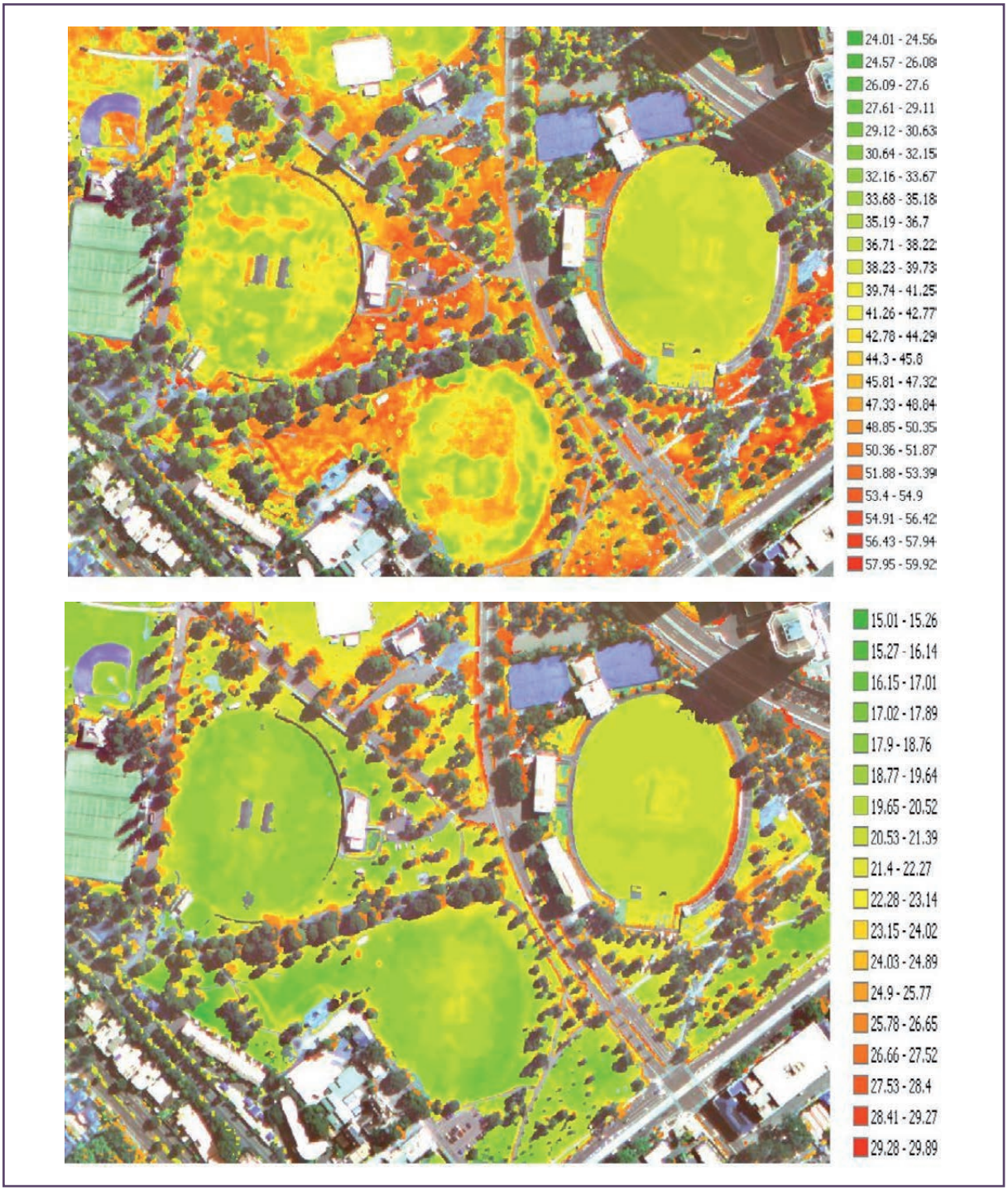

Figure 16: Example of the effects of irrigation in CoPP – irrigated ovals during the day (upper panel) can be clearly seen in contrast with the surrounding non-irrigated grass. At night (lower panel) there is little difference between the irrigated and non-irrigated grass. Please note different scales are used.

LST vegetation relationships – 30 m grid

In order to try to identify relationships between land surface cover and LST, we created a 30 m x 30 m grid across the entire City of Port Phillip area. The percentage cover of each surface type (listed in Table 5) for the 30 m x 30 m grid was defined, including the percentage cover of shadows. Here, we specifically look at the relationships between percentage tree cover, percentage irrigated grass and non-irrigated grass for both the daytime and night-time case. Figure 17 plots the percentage of total vegetation cover with land surface temperature, and clearly describes the reduction in LST as total vegetation cover increases. A more rapid decrease in surface temperature was observed during the day with increasing vegetation cover, suggesting that continued incremental increases in vegetation cover will bring land surface cooling. At night, the reduction in LST is not as pronounced at lower levels of vegetation cover, but where there is around 50 per cent cover or more, the reduction of LST increases. This response is partly due to the absence of solar radiation at night so land surface temperature contrasts are smaller, but also reflects the drivers of the UHI, where natural surfaces cool at a faster rate than urban surfaces. Also, it is not only the plan area fraction of surface cover that is influencing the land surface temperatures, as the 3D nature of the urban environment also influences surface temperatures. In more built up areas (e.g. vegetation cover <50 per cent), urban density increases and high H:W ratios lead to trapping of heat within urban canyons.

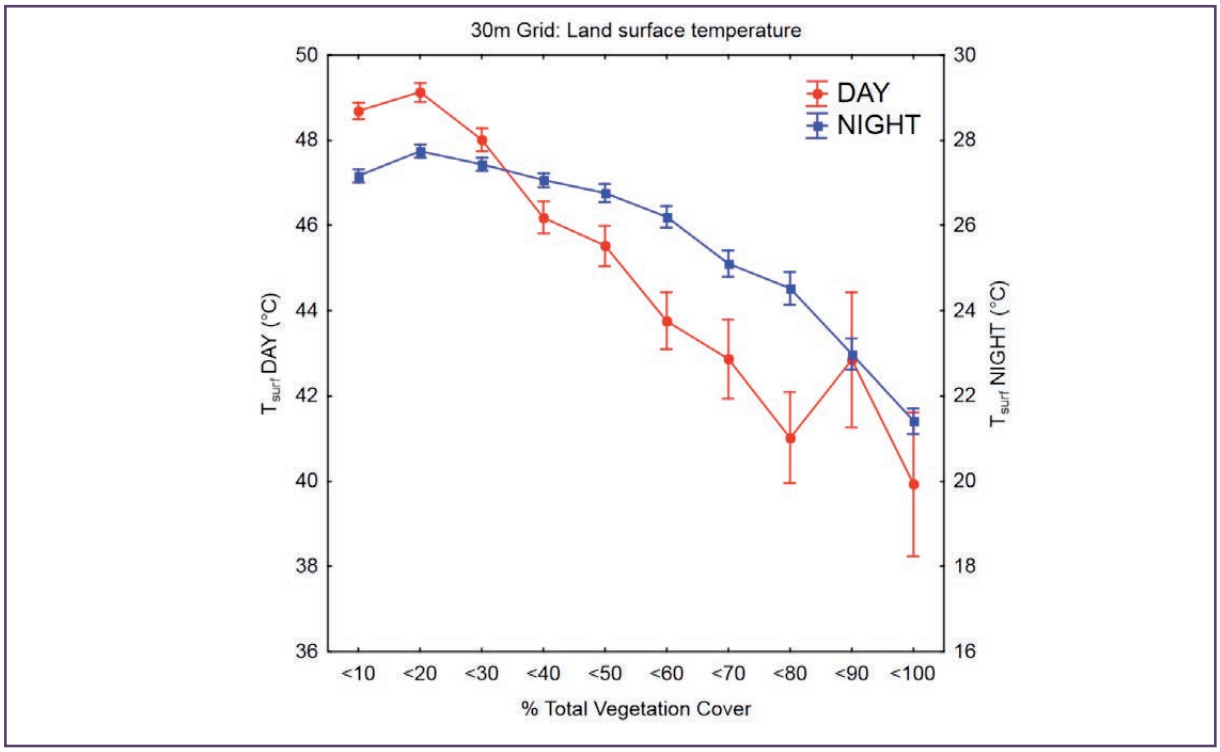

Figure 17: Relationship between percentage of total vegetation cover and land surface temperature for both day (left axis) and night (right axis). Vegetation cover is divided into 10 per cent categories. Error bars denote 95 per cent confidence level.

Vegetation was also separated into its individual components of tree cover, irrigated grass and non-irrigated grass as presented in Figure 18. During the day, increases in percentage of tree cover and irrigated grass cover provided a larger land surface temperature reduction than non-irrigated grass due to evaporative cooling effects and dissipation of heat through the soil. At night, increases in percentage tree cover provided only a small reduction in land surface temperature, while the grass surfaces provided a larger amount of surface cooling. This is most likely due to the location of these surface types and the nature of the surrounding landscape. Grassed areas dominate in parks, which tend to be open and allow uninhibited long-wave cooling of the surface. Meanwhile, the tops of tree canopies remain warm during the evening relative to the rapidly cooling grassed surfaces. This analysis neglects the influence of urban morphology,

due to the biased view of the land surface temperature. Trees may also tend to restrict long-wave cooling at night due to canopy coverage. This was evident in the ground based thermography, where surface temperatures below the tree canopy were relatively warmer than surfaces directly exposed to the sky (discussed below). Nevertheless, it is clear that the amount of green infrastructure has a large bearing on the land surface temperature and will have an influence on the adjacent micro-climate. Trees and irrigated grass were particularly effective at reducing daytime land surface temperatures while at night, grass was more effective than trees.

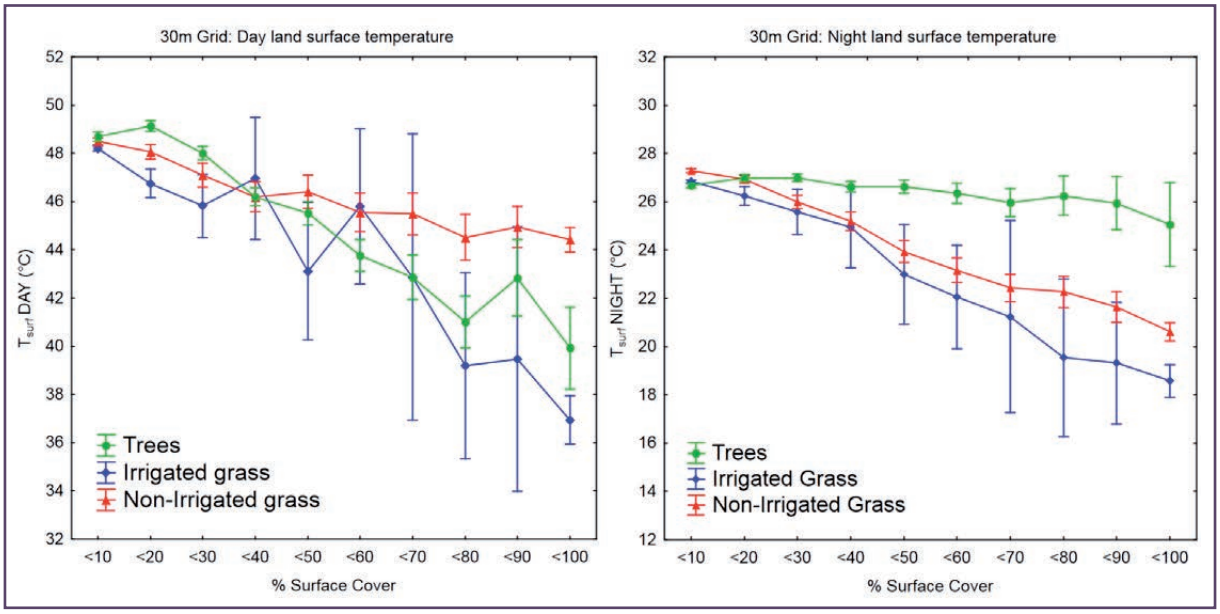

Figure 18: Relationships between per cent tree cover, per cent irrigated grass cover and per cent non-irrigated grass cover with land surface temperature during the day (left panel) and night (right panel), divided into 10 per cent categories. Error bars denote 95 per cent confidence level.

There were limitations with this 30m grid approach due to the presence of shadows. As described earlier, the shadows prevented the assignment of surfaces where they fell and hence no emissivity correction could be applied to these pixels. This means that the LST in shadow, while being cooler due to shading, would have been underestimated too. The larger error bars associated with the irrigated grass in Figure 18 are due to unevenly dispersed patterns of irrigation, so a park that was defined as irrigated would show quite a degree of variability with soil moisture conditions. Also, errors may be due to inaccurate assignment of irrigated and non-irrigated areas, as irrigation patterns may have changed from the time of the image capture used for the land surface classification to when the thermal image was undertaken.

LST vegetation relationships – Urban canyons

Urban canyons represent the spaces between buildings and influence the micro-climate of the surface layer. To counter issues concerning inaccurate surface classifications in the 30 m grid analysis, and to consider the role of urban morphology, further analysis concentrated on the urban canyons in the manually classified focus areas only. The focus here is on the influence of street tree canopy coverage on LST. For the focus areas, polygons were created for each urban canyon and the average land surface temperature calculated to give CANYON T_{surf} (mean LST within the polygon) (Figure 19).

While the tree canopy tops were cooler than urban surfaces during the day, they also provide shading to underlying surfaces. To see if tree canopy cover influenced surrounding underlying urban surfaces, we investigated patterns between *road* surface temperature and tree cover within the urban canyons of the focus areas. The average surface temperature of the road within each polygon gave ROAD T_{surf} was calculated to do this (mean *road* surface temperature only within each polygon).

Finally, we sought to identify under which height to width ratios (H:W) tree cover was most effective in cooling urban canyons. We hypothesised that increasing height to width ratio of the urban canyon would increase shading of the canyon during the day from buildings, limiting the effectiveness of shading from vegetation in surface cooling. This will help identify priority H:W for implementation of street trees. For each urban canyon, the average street width and the average building height were collated using the LiDAR data.

Figure 19: Example of a street canyon polygon (left panel) within the Middle Park focus area. CANYON T_{surf} was the average surface temperature for the whole canyon (centre panel) and the ROAD T_{surf} was the road surface temperature only within the polygon (right panel).

The aim was to understand the influence of tree canopy coverage on overall CANYON T_{surf} and ROAD T_{surf}, and under what H:W arrangements is tree cover most effective. Table 6 presents regression coefficients between per cent tree cover and land surface temperature under different H:W and identifies when the influence of per cent tree cover was statistically significant (red and bold numbers in Table 6). For instance, during the day, tree cover had a statistically significant influence on overall CANYON T_{surf} when the H:W < 0.8, showing a negative correlation with CANYON T_{surf}. A negative correlation means that as per cent tree cover increases, CANYON T_{surf} decreases. When H:W > 0.8, the influence of tree cover was reduced and no longer statistically significant. Therefore, trees were most effective in wide, open canyons. This does not mean that increasing tree cover did not reduce surface temperatures in canyons with H:W, it just means trees were less effective. There are multiple factors that are influencing surface temperatures at any one time (e.g. surface materials, total imperviousness), but this analysis attempts draws out when the influence of per cent tree cover was most significant and hence should be prioritised. Trees become less significant in surface cooling as H:W increases because the influence of buildings becomes more pronounced.

Table 6: Regression coefficients between CANYON and ROAD surface temperature with per cent tree cover for different height to width ratios (H:W). Negative numbers present a negative correlation (reduction in surface temperature) and red and bold numbers are statistically significant. The number of observations is given by *n*.

Per cent tree cover					
		CANYON T_{surf}		ROAD T_{surf}	
H:W	*n*	DAY	NIGHT	DAY	NIGHT
< 0.4	81	**-0.79**	**-0.52**	**-0.46**	-0.03
0.4 - 0.8	50	**-0.51**	0.1	0.16	0.119
0.8 - 1.2	25	-0.14	0.102	-0.13	0.034
1.2-1.6	21	-0.14	0.073	-0.37	0.119
1.6-2.0	19	0.372	-0.01	0.216	0.021
<2.0	19	0.05	0.134	-0.18	0.251

Using the information in Table 6, Figure 21 presents plots of land surface temperature (CANYON T_{surf} and ROAD T_{surf}) versus per cent tree cover to demonstrate the reduction in surface temperatures as tree cover increases when the H:W < 0.8. Similar to the patterns seen in the 30 m grid analysis (Figure 18), increasing tree canopy coverage led to a reduction in the average CANYON T_{surf} during the day and to a lesser extent at night. The tree canopy tops were cooler than the surrounding urban land surfaces, so the land surface temperatures were reduced (as viewed by the thermal camera). With regards to ROAD T_{surf} there did not appear to be any reduction until tree cover was >40 per cent as below this level the canopy shading was not large enough to shade the road. At night, there was no difference in road surface temperatures. Offerle et al., (2007) has noted that that heat release from walls is the dominant source of sensible heat fluxes (atmospheric heating) at night, which highlights that airborne thermal imagery cannot actually 'see' the main source of night time atmospheric heating.

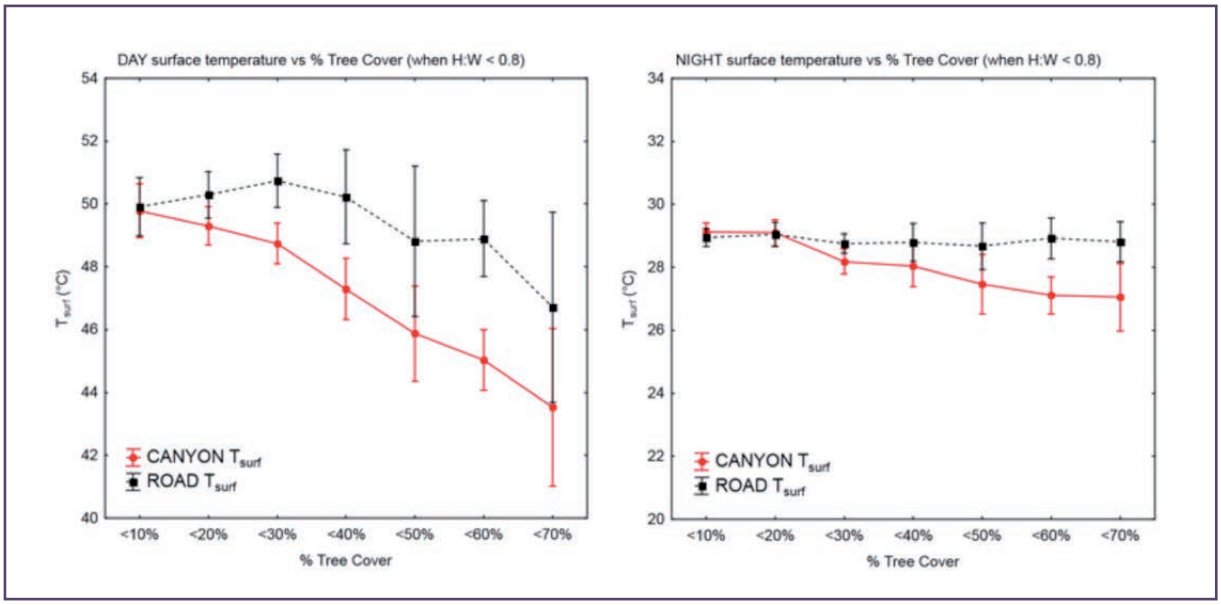

Figure 21: Relationship CANYON and ROAD land surface temperatures and per cent tree cover (a and b - upper panels) and Height to Width Ratio (H:W) (c and d - lower panels) during the day (a and c) and night (b and d). Error bars denote 95 per cent confidence level.

The focus on ROAD surface temperatures did not show as large an effect as expected, but this is explained by the fact that the daytime flight was undertaken at solar noon when shading was minimal. This highlights a limitation in this analysis. These data present just two points in time over the course of the day: solar noon and night. Shading will change significantly during the day and influence land surface temperatures, and the night time surface temperatures could still be more of a result of afternoon shading patterns, especially in north-south oriented streets. To reiterate, the thermal image is only a plan view of the surface and neglects the surface temperatures of walls. Nevertheless, the key focus here was on green infrastructure, and the analysis has shown a clear influence of street trees on surface temperatures, and for urban cooling purposes, it is important that street trees are strategically placed to maximise surface cooling during the day.

Unfortunately, sample size (*n*) was also a limiting factor in this analysis, as data can only be taken from existing canyon arrangements. Figure 20 highlights the predominant types of canyon arrangements and obviously, vegetation is mostly found in wide open streets where H:W ratio is low, so it makes sense that vegetation cover has a significant influence on land surface temperature. There were few samples where tree cover was high in streets where H:W were high. Limitations in space or presence of infrastructure may prevent the implementation of street trees. A larger area of analysis could increase the sample size, but creating the canyon polygons in GIS is a manual exercise and takes time to complete, and this analysis also requires an accurate land surface classification that was only available for the focus areas. The limit in sample size also means there were not enough samples to assess the influence of street canyon orientation.

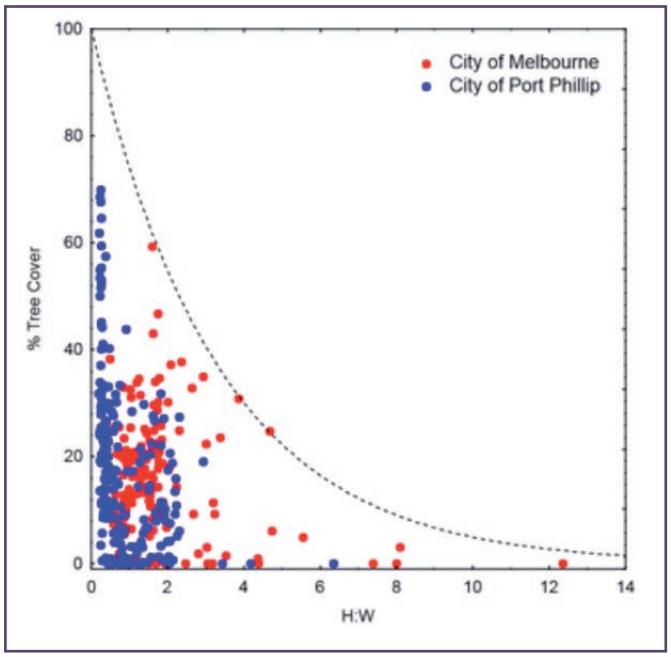

Figure 20: Relationship between per cent tree cover and H:W within urban canyons of the CoPP focus area and selected areas of CoM.

Information on strategic placement for surface temperature reductions can be drawn out from the thermal imagery (e.g. Figures 22 and 23). Examination of the daytime thermal imagery revealed:

- surface temperatures tended to be higher in wide open streets, as well as open urban areas such as car parks
- the southern sides of streets were warmer than the north sides of streets due to larger amounts of solar radiation
- when street canyons were oriented east-west, and H:W ratios were approximately one, around 25-30 per cent of the street canyon floor was shaded
- tree canopies produced surrounding areas of shade.

While surface materials will play a strong part in land surface temperatures, the amount of solar radiation received by a surface is one of the most dominant controllers. The amount of shading from a building can be estimated through simple trigonometry and can help inform where vegetation is needed most. For instance, for an east - west oriented street canyon, when the sun angle is 75° during summer, if the H:W reaches as high as three, around 80 per cent of the street canyon floor will be shaded. Under such circumstances, this area would not be prioritised for tree implementation; the priority should be given to wide open streets where there is little shade and high land surface temperatures. The urban canyon analysis shows that street trees should be placed in urban canyons with H:W < 0.8 and a tree cover > 40 per cent is necessary.

Figure 22: Example of road surface temperatures in Middle Park during the day.

Figure 23: Example of road surface temperatures in South Melbourne during the day.

3D land surface temperatures

Night time land surface temperatures were also observed using ground based thermography at the time of the night-time thermal flight for CoPP on the night of 25 February 2012. This was done to complement the airborne thermal imagery. Examples of the ground based thermography are presented in Figure 24. Figure 25 presents 360° views from points within the urban canyon at four locations for comparison with the airborne thermal remote sensing. These images highlight some interesting points, but the images apply an emissivity of 0.98 to the whole image, and may also show the effects of thermal anisotropy (the property of being directionally dependent) (e.g. road surface temperatures appear to reduce with distance away from the camera), and should only be considered in a relative sense. Some general findings from examination of the ground based thermography showed:

- the walls of urban canyons remained relatively warm at night compared to the street canyon floor, further highlighting the role of walls in night time atmospheric heating, as noted by Offerle et al., (2007)
- as with the airborne thermal remote sensing imagery, there was no clear indication that canyon H:W had any influence on the road surface temperature at night, and factors such as road surface materials may have had a more dominant influence
- Western and Northern facing walls were the warmest, due to surface heating during the hottest part of the day and these are the walls receiving sunlight prior to sunset and so remain the warmest when the thermal imagery is taken
- covering surfaces restricts long-wave cooling at night. This is evident under tree canopies where road surface temperatures were slightly higher than in more open streets, and also under cars where radiative temperatures of surfaces remain high. Sky view factor (defined as the percentage of viewing hemisphere that is unobstructed to the open sky) may be a better measure than H:W, as it takes into account all obstructions to long-wave cooling (e.g. trees), not just buildings.

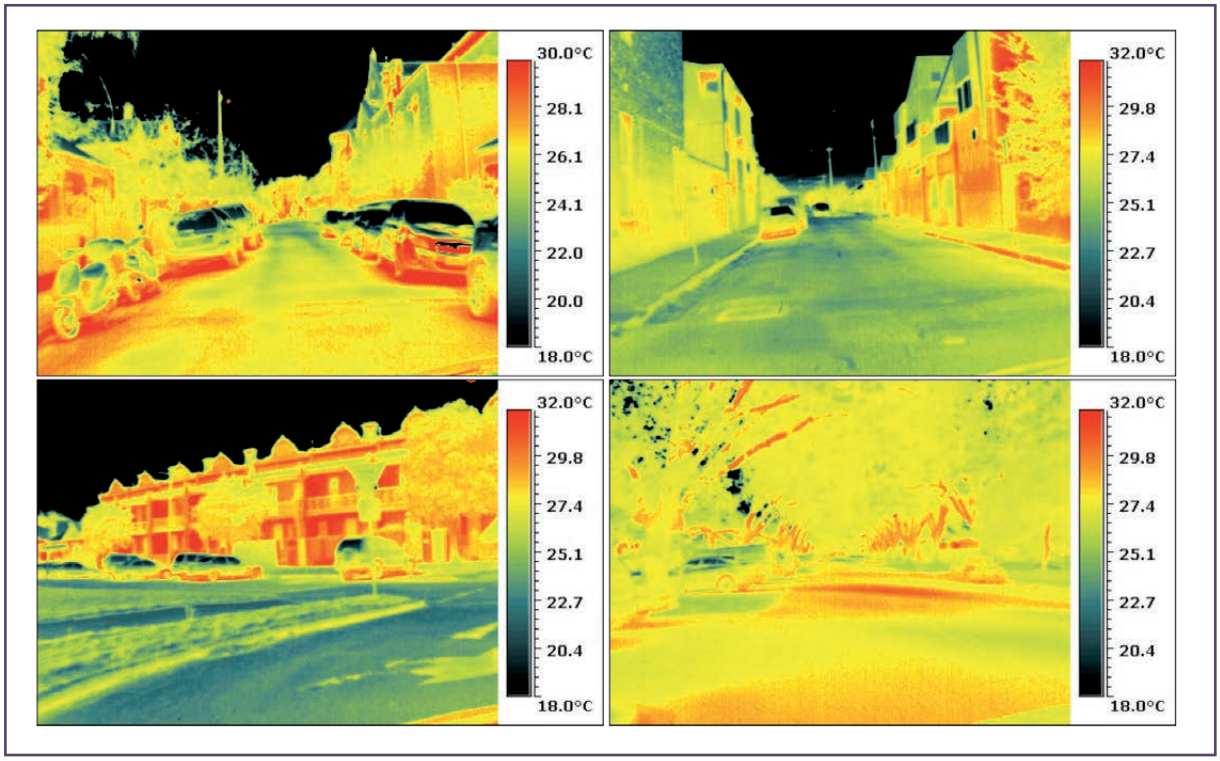

Figure 24: Example images from the ground based thermography of locations within the CoPP on the night of 25 February 2012.

The trapping of long wave radiation by tree canopies as highlighted by the ground based thermography could lead to slightly warmer air temperatures within the urban canyon. Tree canopies themselves have a moderating effect on surrounding air. However, this does not necessarily mean that air temperatures are higher beneath tree canopies at night as shading during the day results in less heat being stored in the urban fabric during the day for release at night, meaning overall air temperature could be lower. Further research is needed in this area that considers heat fluxes into the urban fabric of urban canyons and the effects of surrounding trees.

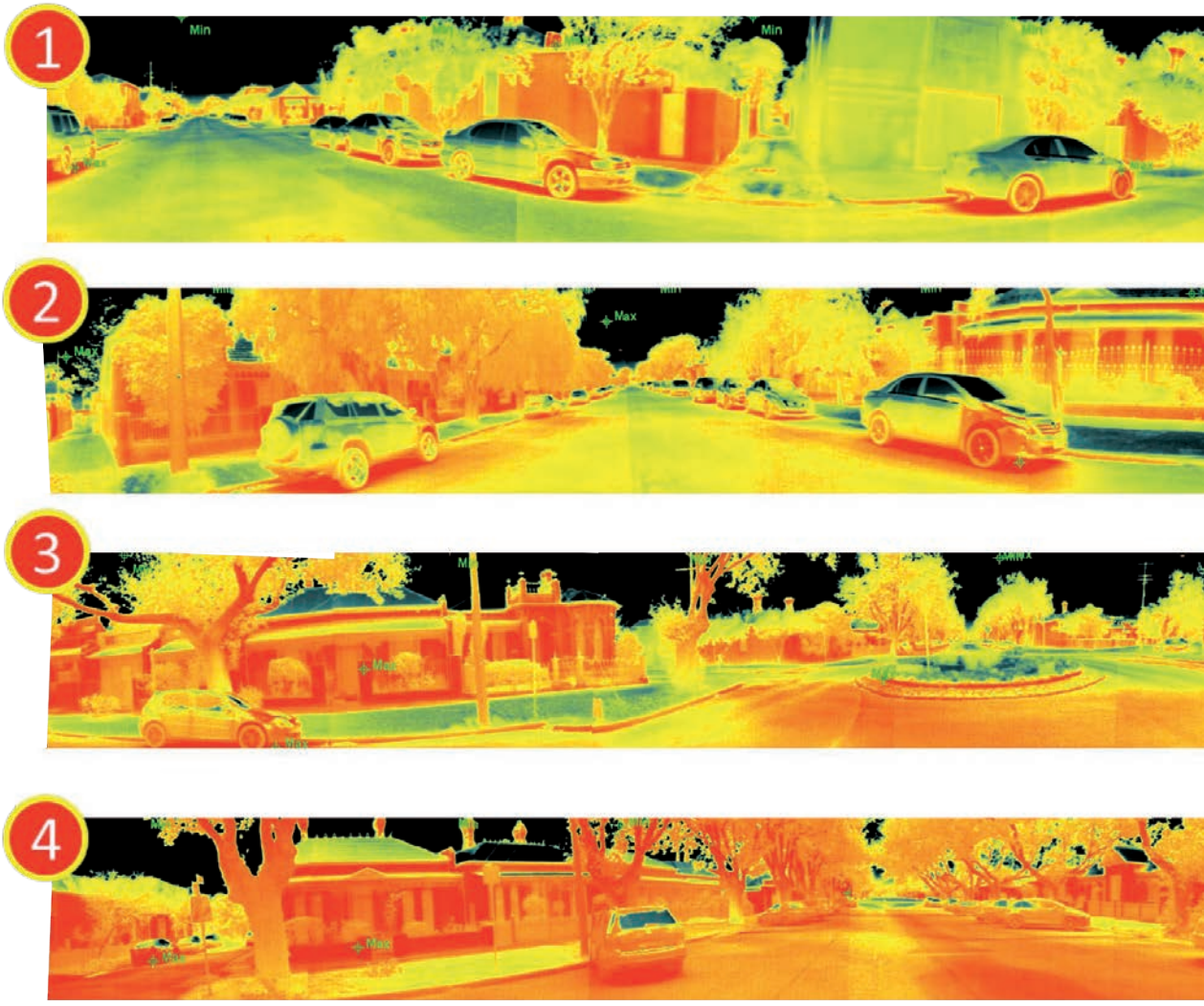
1
Min
Min
2
Max
Max
3
Max
4
Max


3
1
4
2

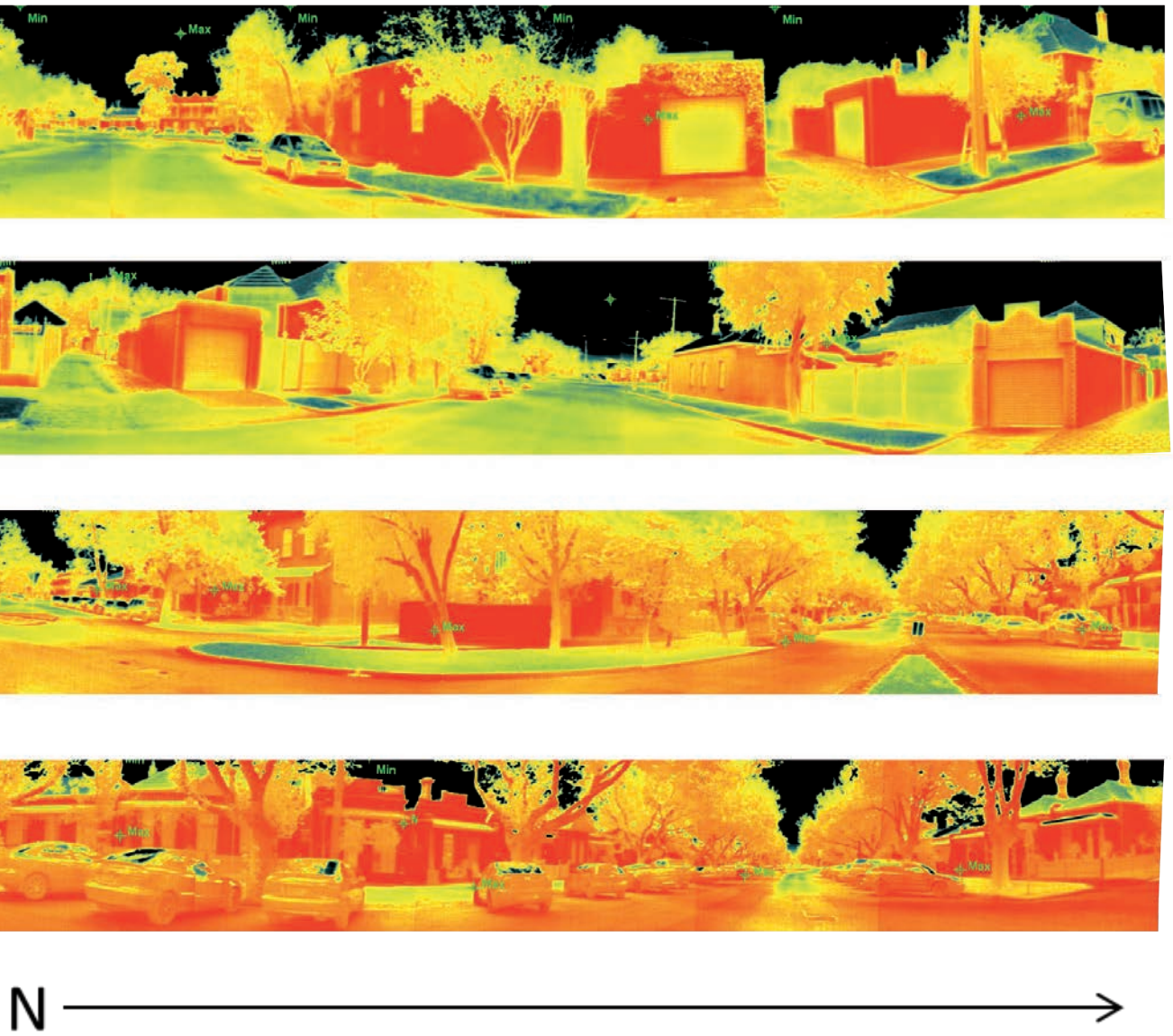

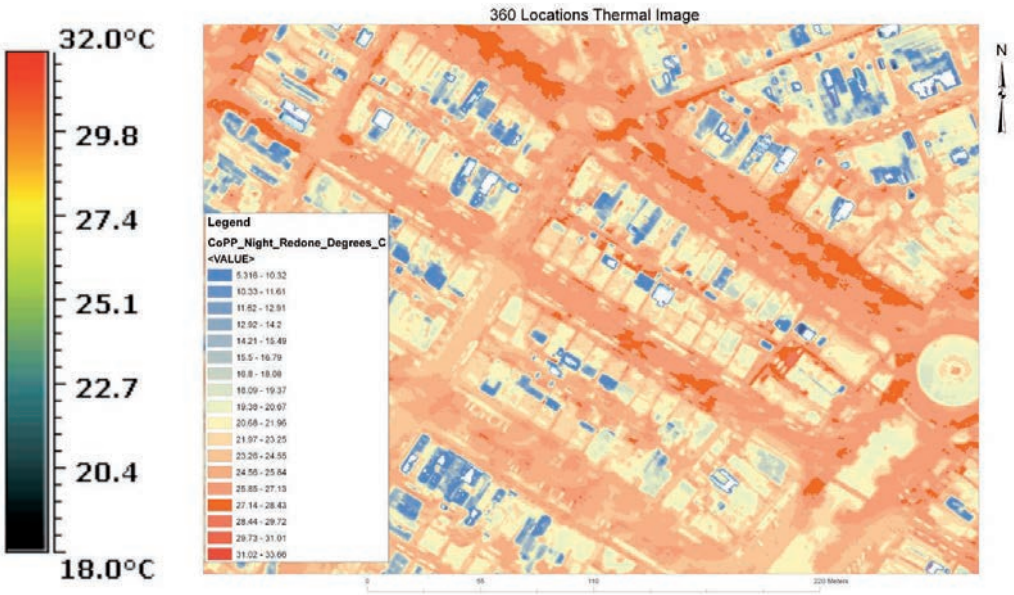

Figure 25: 360° thermal images at four locations in urban canyons in CoPP on 25 February 2012. Images apply a standard emissivity of 0.98. A plan view thermal image is also provided which is also applies a single emissivity of 0.98 to allow comparison.

Land surface - air temperature relationships

Airborne thermal remote sensing is used as a tool to rapidly map LST across a wide area. Governments are keen to map hot-spots to help identify key areas for risk management, but it is air temperature that is the main variable of interest. The local scale MODIS data identified that patterns in land surface and air temperatures were similar under these conditions. In this analysis, the micro-scale air temperature data collected at the time of the flights was compared with the high resolution thermal imagery. The air temperatures observed during the transects for both the CoM and CoPP can be viewed in Appendix D and highlight how air temperatures can vary by several degrees (+4°C) within a single council municipality. Air temperatures broadly followed expected patterns with higher temperatures observed in more densely built up areas with little vegetation, while parkland areas were several degrees cooler.

As identified above, LST can vary significantly within an urban canyon during the day depending on land surface type and the amount of shading from tree canopies and buildings. During the CoM night time flight, Monash University had ten micro-climate stations installed in Bourke St, Melbourne. This provided a high resolution comparison between land surface and air temperatures at night at the time of the flight (Figure 26). While there are too few points to derive any meaningful relationships, visual inspection of Figure 26 demonstrates that land surface and air temperatures follow similar patterns: cooler temperatures on the northern side of the canyon due to shading during the day; and some cooling as a result of tree shading. Of course, these data were collected under a very specific set of atmospheric conditions (e.g. low wind, clear skies) and will vary temporally.

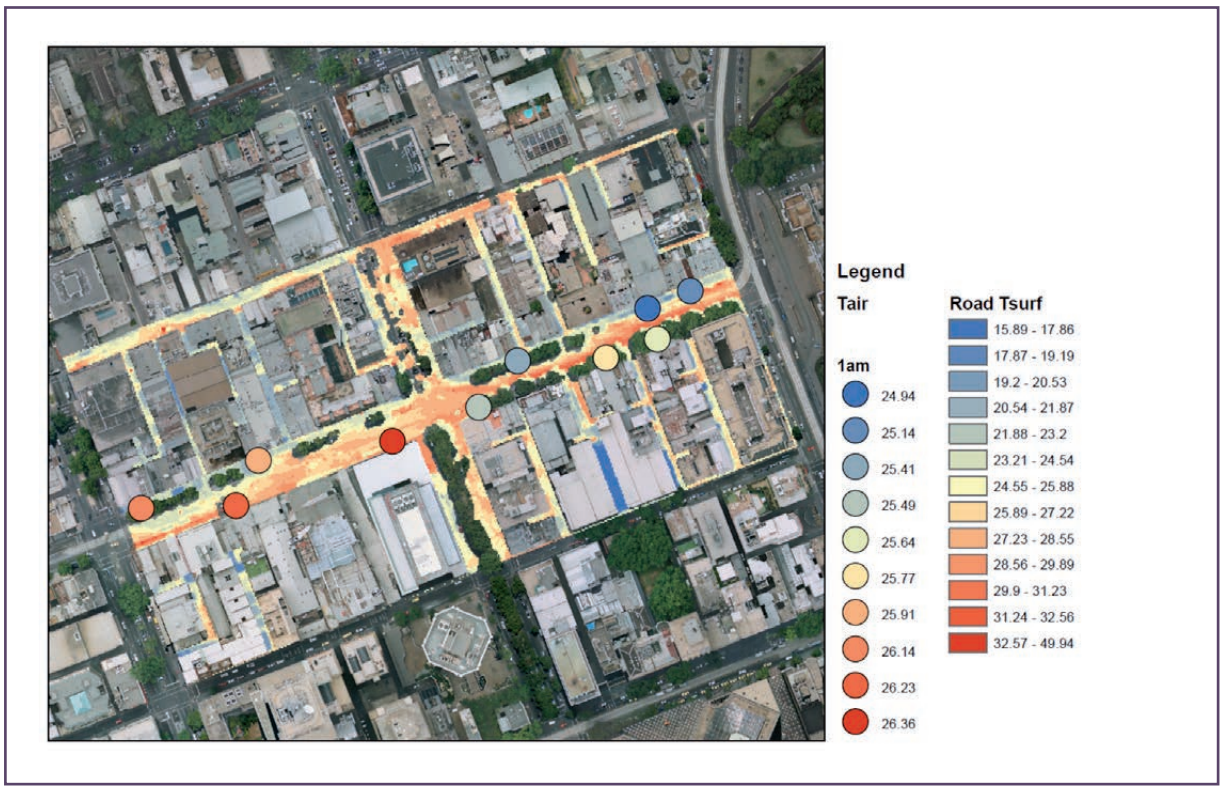

Figure 26: Comparison of road surface temperatures (corrected to 1am) (thermal flight) and air temperature (micro-climate station) in an urban canyon in Bourke St, Melbourne at 1am. Wind direction was Northerly at the time and <1 m/s. Road surface temperature is not corrected for emissivity.

In truth, it is more difficult at the micro-scale to link land surface temperatures to air temperatures than it is at the local scale. Air temperatures at a point in the urban canopy layer are influenced by the background meso-scale synoptic conditions and regional airflows, local-scale airflows, adjacent micro-scale LSTs and anthropogenic heating and cooling. Trying to link air temperatures directly to land surface temperatures at this scale is highly problematic. Determining the 'footprint' of the land surface that influences air temperatures at a particular point is extremely difficult as it continually changes, as does its relative influence on air temperature compared to larger scale air masses. Computation fluid dynamics (CFD) modelling could help determine micro-scale footprints, but this is extremely expensive.

This issue is outlined in Figure 27 which presents the data from the air temperature transect taken in the CoPP on the night of 25 February 2012. Air temperature (T_{air}) was measured every second, and averaged into 10 second periods. At each 10 second period, a 15 m radius buffer was placed around the point in GIS software from which the average land surface temperature was estimated. A 15 m buffer was chosen to align with the common street canyon width. Land surface temperatures of these 15 m buffers were extremely variable (Figure 27) and it is difficult to observe any trends with air temperature and a statistically significant correlation between T_{surf} and T_{air} was not present. To try and achieve a better representation of the how the land surface influences air temperature, an average of the previous six points (i.e. 1 minute) for LST was taken (Figure 27). A linear regression analysis showed a statistically significant correlation and broad similarities between T_{surf} and T_{air} for within canyon air temperatures. However, this began to break down in areas that were more open, as the air temperature became increasing influenced by the local scale air masses. This was particularly evident for air temperatures observed adjacent to the coast in CoPP where sea breezes were likely to have a stronger influence on air temperature than the land surface (Figure 27: approx. 12.31am to 12:42am). This highlights the influence of urban morphology on micro-scale air temperatures, where deep urban canyons limit ventilation and the surface has a more dominant control on the air temperature. These issues also limit the ability to determine percentage of tree cover influencing air temperatures at the micro-scale, and no clear relationships could be found.

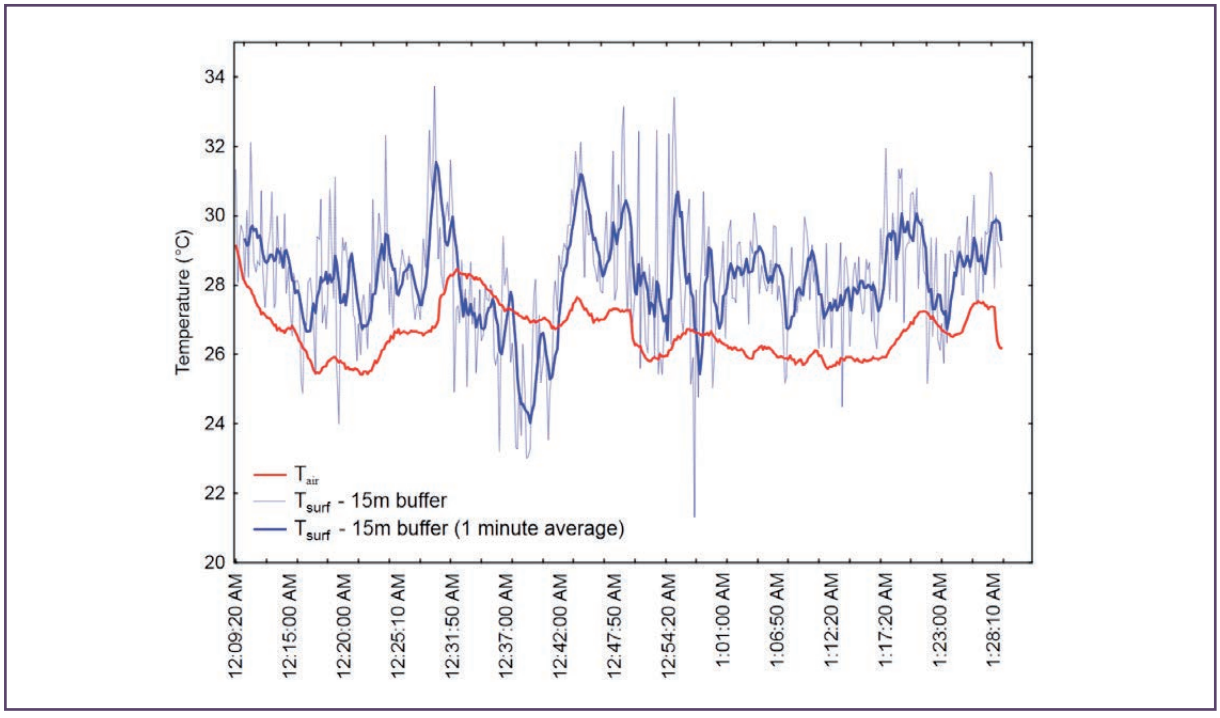

Figure 27: Plot of air temperature (10 second average) and land surface temperature using instantaneous 15m buffer and 15m buffers over the equivalent of 1 minute of travel for the air temperature transect on 25 February 2012.

Figure 27 also highlights again quite a difference from the cross city transects conducted on the same night. MODIS-derived LSTs were lower than the observed air temperatures (Figures 12 and 13), while here, T_{surf} derived through the higher resolution airborne thermal remote sensing was mostly higher than T_{air}. This again emphasises the influence of scale in urban climates. A range of buffer sizes was also examined in this study and suggested that as the buffer size increased, the LST decreased. This highlights the complexity of trying to quantify variations in urban air temperatures via remotely sensed data (Tomlinson et al., 2011).

3.3 Temporal variations in surface temperature

The airborne thermal remote sensing data provides a snapshot of surface temperatures at a particular point in time. The ground based stations that were established during the campaign allow for an examination of variations in surface temperature over the diurnal course. Figure 28 presents a monthly average (9 February 2012 – 8 March 2012) of the general differences in surface temperature from the ground monitoring stations. Urban surfaces (concrete, asphalt) were warmer than natural surfaces (grass, bare soil) over the entire diurnal course. Irrigation of grass surfaces lowered the surface temperature and this effect was most pronounced during the day as a result of surface cooling through evapotranspiration (Figure 28). The maximum daily surface temperature of the irrigated grass was around 5°C cooler than the non-irrigated grass over this period. During the day, the surface temperature of the concrete site in the CoPP (site located at the South Melbourne Market) was lower than the temperature of the concrete observed at the CoM site. This was because cars were sometimes parked within the field of view of the sensor at this site, but at night time the data were not affected. Water showed only a small diurnal range due to its large thermal capacity, so it is very cool during the day but remains warm during the night. Despite this variation, water was still similar or cooler than urban surfaces (e.g. concrete) at night.

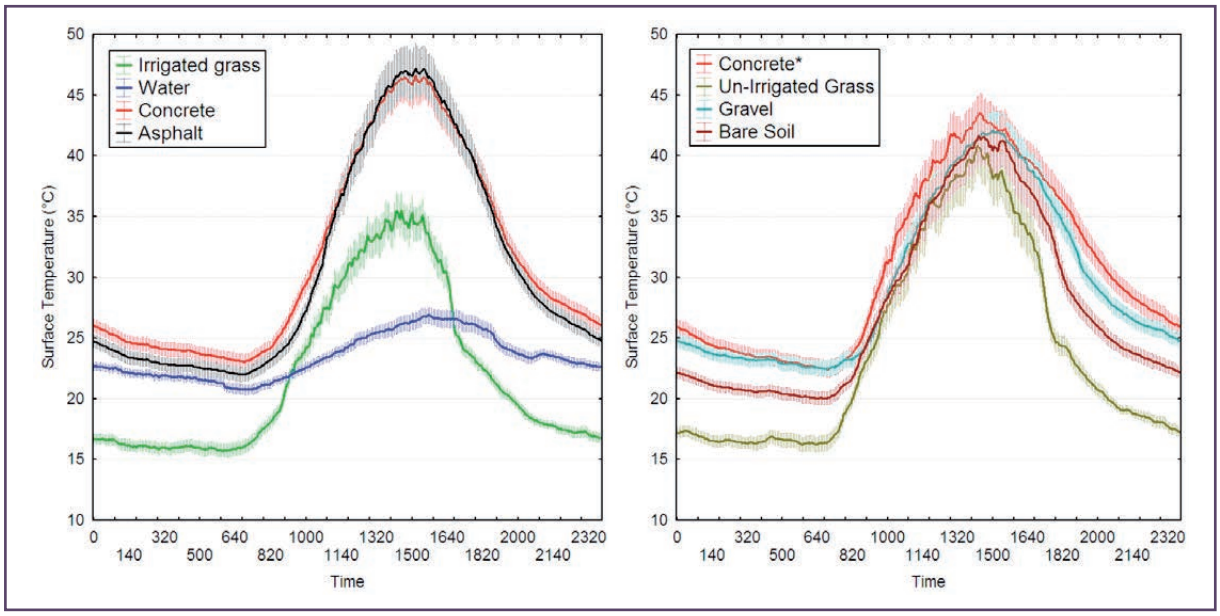

Figure 28: Surface temperatures from ground based monitoring stations located in the City of Melbourne (left panel) and City of Port Phillip (right panel) averaged over a month long period from 9 February 2012 – 8 March 2012 (Concrete site in CoPP was not isolated and cars could park during the day).

Given the importance of emissivity in determining surface temperatures, we also established ground monitoring sites on three rooftops of galvanised steel: one rooftop at Melbourne University (CoM); a second on the City of Port Phillip (CoPP) council building rooftop; and a third site on a rooftop at Monash University to allow for further comparison. Figure 29 presents average monthly surface temperatures (9 February 2012

– 8 March 2012) for these rooftops sites, with all three sites corrected for an emissivity value of 0.86. Clearly, there were significant differences in surface temperatures. This difference is primarily a result of a single value for emissivity for all three roofs and highlights the challenges faced when correcting airborne thermal remote sensing data. Surface temperatures of the CoPP Council rooftop were very low, so this rooftop was likely to have a very low emissivity (e.g. could be as low as 0.3 for instance). Furthermore, the low emissivity of the CoPP council roof means that a large proportion of incoming long-wave radiation (e.g. from clouds) is reflected off the rooftop, and this is seen by the sensors (and incidentally, also by any airborne thermal remote sensing camera) which results in errors. This is demonstrated in Figure 30, where the surface temperature of the CoPP Council Roof closely tracks the amount of incoming long-wave radiation (measured at Monash University), whereas this is not the case for other surfaces with a high emissivity (e.g. > 0.9) (not shown).

Clearly, the influence of emissivity is complex and makes analysing and interpreting airborne thermal remote sensing data difficult. To achieve accurate values, corrections would also need to be made for reflected long-wave radiation and we investigated this, but were unable to improve the results. Monitoring equipment like thermal cameras simply cannot account for this, and as such, surface temperatures for surfaces with low emissivities are virtually meaningless. However, during an airborne thermal remote sensing flight focussed on urban heating, skies should ideally be clear so the effect of reflected long-wave radiation would not be a problem. However, to accurately correct for emissivity, this would have to be measured for each individual surface – but emissivity measurements are notoriously difficult to measure and are highly variable. Nevertheless, corrected surface temperatures of natural surfaces and ground level urban surfaces like asphalt are likely to be more accurate and emissivity values have a smaller variability across these surfaces.

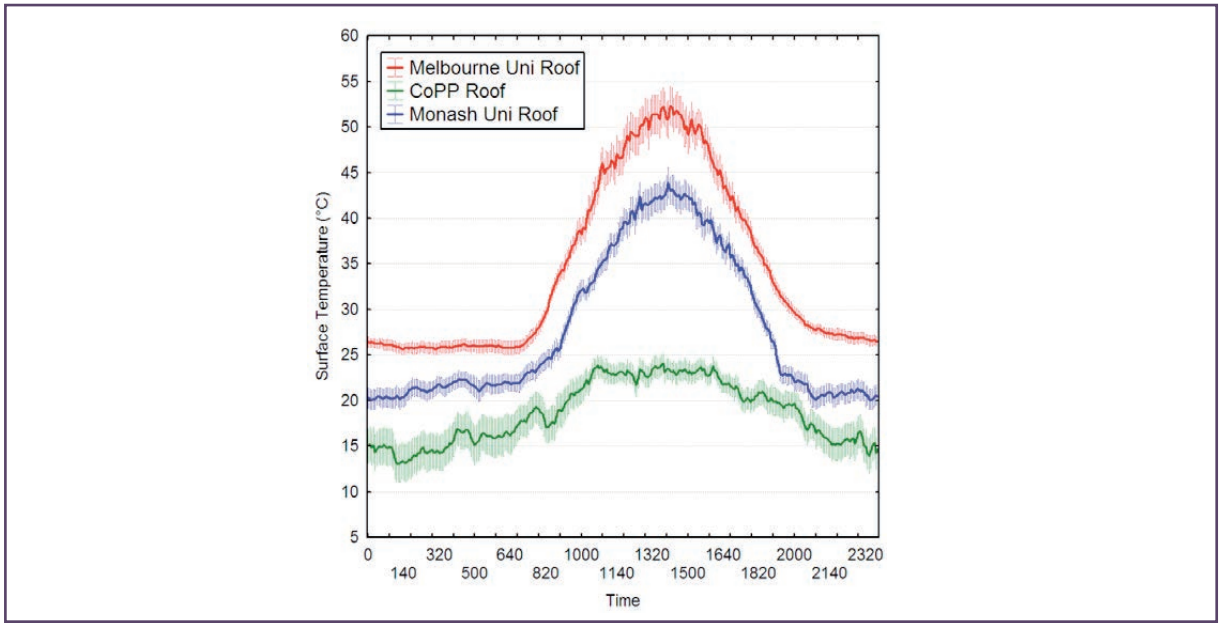

Figure 29: Presents the surface temperature of three different galvanised steel roofs, using a constant emissivity value of 0.86 over a month: 9 February 2012 – 8 March 2012.

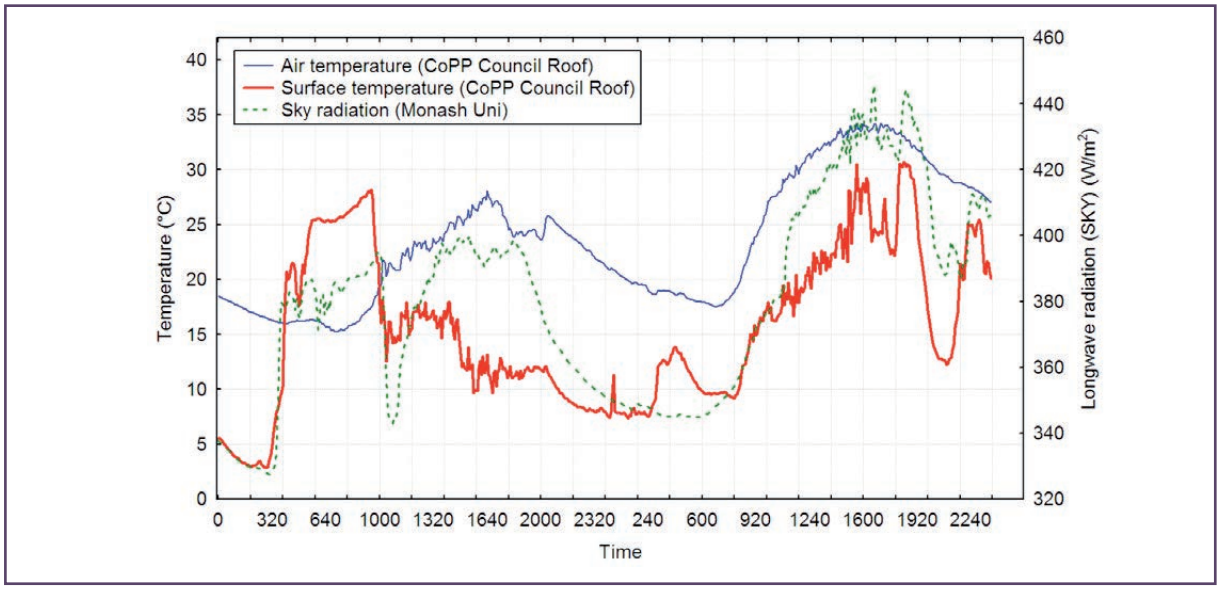

Figure 30: The influence of reflected long-wave radiation from the sky on remotely sensed surface temperature for surfaces with low emissivity: 14 – 15 February 2012.

3.4 Building scale effects of vegetation

Using ground based thermography, thermal images of a green roof and a green wall (green façade) were collected (Figure 31). These images assume a constant emissivity of 0.98 and surface temperature should be viewed in a relative sense. While the thermography is by no means an extensive analysis of thermal effects of green roofs and walls, it provides a brief insight into their effects on land surface temperature during the day.

For the extensive green roof located at Monash City Council, surface temperatures were very high during the peak daytime heating period. The roof soil was a coarse scoria based soil, and was covered with a layer of dark stones which tended to heat up during the day. Vegetation types were generally succulent varieties, which do not freely transpire during the day to conserve water. Plant coverage was also not especially dense, so much of the soil surface was exposed and the dark surface stones heated up and showed surface temperatures that were similar to the adjacent galvanised steel roof. Some plant species were under stress and there were signs of die-back in areas. This roof would benefit from a lighted coloured soil substrate to increase the surface albedo, increased plant coverage and an irrigation regime to help promote evaporative cooling (Lundholm et al., 2010) and plant survival. MacIvor et al. (2011) suggest that roof surface temperatures are an important indicator of thermal performance and a reduction in a surface temperature is likely to lead to a reduced heat flux into the building.

The green wall (façade) located at the Corkman Pub showed large temperature reductions in comparison with the adjacent building materials (red and white painted brick) and the asphalt pedestrian path. Surface temperatures of the green wall were as much as 15°C cooler than the red painted brick wall. The effects of albedo on surface temperature can also be seen where the areas of white paint were as cool as the vegetation of the green façade. The reduction in surface temperature is likely to reduce heat fluxes through building walls (Wong et al., 2010).

It is clear that the design of green infrastructure is critical. In the case of the green roof, it is not likely that this roof was providing much benefit in terms of the outdoor thermal environment. Planting density, species type and irrigation regimes will all influence the effectiveness of green infrastructure (including trees and grass) and more research is needed to investigate the optimal designs of green infrastructure across Australian urban environments.

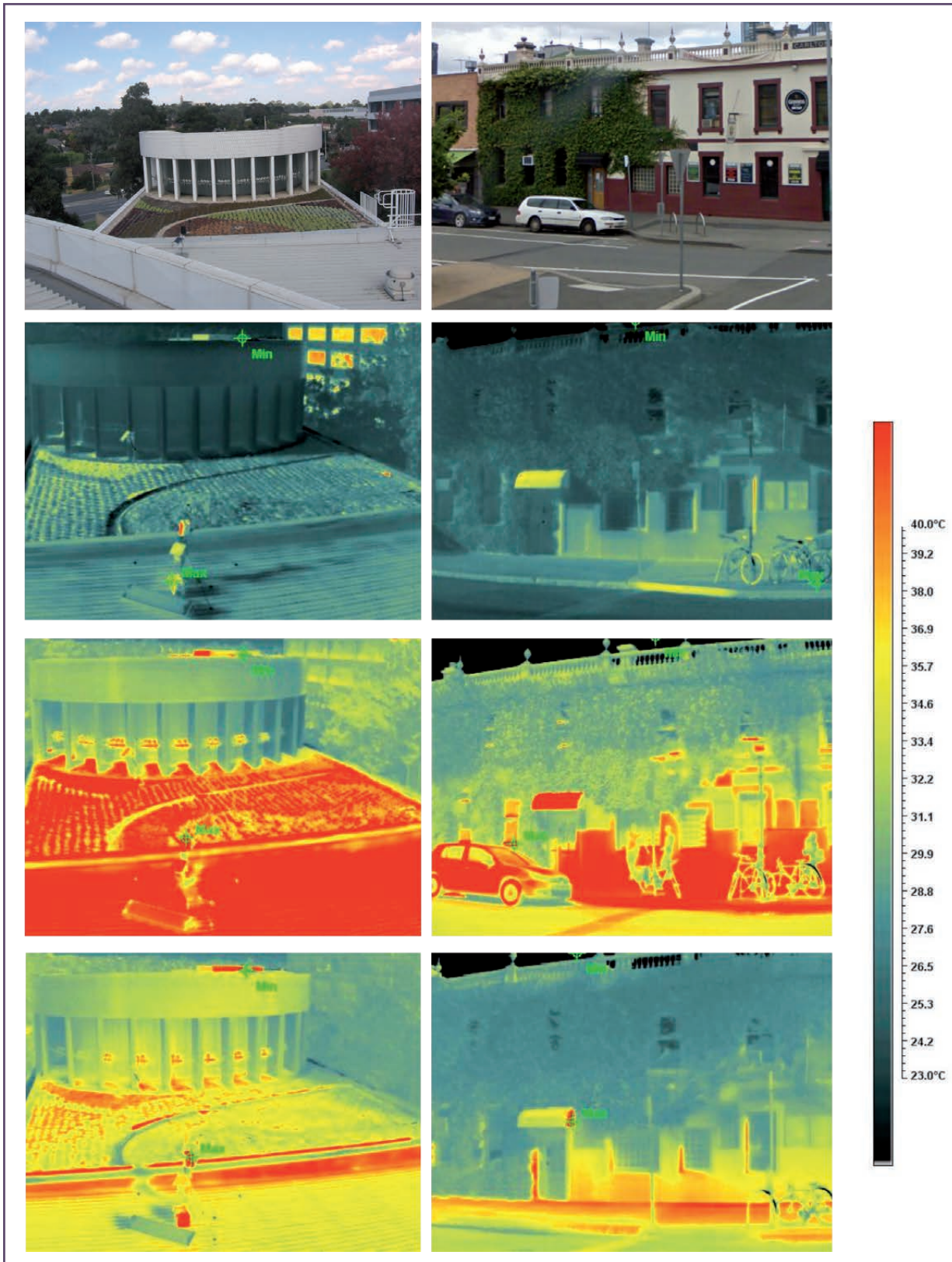

Figure 31: Selected thermal images of the green roof on the Monash city Council building roof (left images at 10.10am, 2.05pm and 5.30pm) and the green façade at (right images at 9.15am, 1.00pm and 5.30pm).

4. Conclusions and policy implications

This project drew on a wide range of data sources and collaborations between researchers and government organisations. This presented a unique opportunity to undertake analysis of the value of airborne thermal remote sensing for policy development in mitigating excess urban heat. It also presented an opportunity to understand the role of green infrastructure in reducing land surface temperatures.

4.1 Practical application of airborne thermal remote sensing

A review of literature and discussions with state government and local councils revealed the kind of applications that airborne thermal remote sensing might be used for:

Identifying hot-spots across the landscape

Key uses of the thermal mapping were the identification of hot-spots in the landscape and as an excellent communication tool for government and industry. This can help in identifying areas for intervention across the landscape and can be used in conjunction with data on population vulnerability based on factors such as age, to map high risk areas in terms of human health. The high resolution of airborne thermal remote sensing means that surfaces with extreme surface temperatures can be identified such as particular streets that may show intense surface heating or restricted cooling. High resolution thermal mapping can provide information on important landscape design features, such as which sides of the street are warmer, the effect of individual tree canopies, or areas where additional irrigation might be needed. This can help prioritise where interventions should be targeted to reduce surface temperatures at the micro-scale. The key assumption here is that a reduction in surface temperature will lead to reduced sensible heating of the atmosphere and as such, will lead to reduce canopy layer air temperatures.

As this work has shown, there were certainly similarities between patterns of land surface temperature and air temperature, but no conclusions could be drawn of the relative magnitude of air temperature reductions. Furthermore, it appears that scale is important when considering surface and air temperature relationships, with surface temperatures detected by the coarse resolution MODIS data being several degrees cooler in comparison to the air temperature, while the higher resolution airborne thermal remote sensing surface temperatures were closer to the air temperature. This is likely due to different methodologies employed to collect the data, but the coarser resolution of MODIS also means that the data is a mix of land surface types, including natural surfaces which tend to be cooler. Nevertheless, airborne thermal remote sensing can be used as a proxy for identifying hot-spots, but according to (Tomlinson et al., 2011) in their review of remote sensing techniques for UHI analysis, *"a significant research gap still exists which is the quantification of the relationship between measured air temperatures and remotely sensed LST data"* (pg. 303). This is evidenced here in this study too, and must be acknowledged as an uncertainty when using remotely sensed land surface temperature data to inform policy.

Assessing building energy efficiency

Another use of high resolution airborne thermal imagery is to identify poor performing buildings in terms of heat loss/gain and hence energy efficiency. However, airborne thermal remote sensing has limits with respect to this purpose for several reasons.

1. Given the large proportion of galvanised steel roofs and similar building materials, along with the uncertainty in emissivity values, it is not possible to determine whether a hot or cold roof represents a building that performs well in terms of energy efficiency for these types of roofs. The thermal camera cannot adequately capture surface radiometric temperatures for surfaces with low emissivity. The cool roof could represent either a building that performs well, or it could be an artefact of the data collection method.

2. Thermal mapping provides for the calculation of rooftop surface temperatures and while a hot roof is largely a result of a large amount of net available energy at the roof surface, it does not necessarily mean the building is performing poorly in terms of energy efficiency. A building's thermal performance will have as much to do with its insulation and design, as with the surface temperature of the building's rooftop.

3. Only a plan view of the building can be seen using airborne thermal remote sensing, while building energy efficiency relates to the whole building envelope, including walls and windows which may have good thermal performance.

Trying to identify poorly insulated buildings or high energy consumption buildings using airborne thermal remote sensing has limited value. What is of value is the identification of rooftops that are *relatively* hot and could be prioritised for cool roofs or green roofs to reduce the contribution of the rooftops to sensible heating of the atmosphere (recognising the limitation of the data). The application of 'cool roof' technologies (e.g. highly reflective paints) can serve to reduce roof surface temperatures as a result of reduced net available energy at the surface and atmospheric heating (Coutts et al., 2012).

Relationships between land surface temperature and surface characteristics

This project has demonstrated the relationships between land surface temperature and land cover. The focus here has been on vegetation, highlighting the clear role of vegetation in reducing land surface temperatures, particularly during the day. When considering the 30m grids for the CoPP, results suggested that for a 10 per cent increase in total vegetation cover, in general there was around a 1°C reduction in land surface temperature during the day (under study conditions). This demonstrates the value of airborne thermal remote sensing when used in combination with other data layers produced from other remote sensing products. The comparison of broad surface types for the CoPP clearly identifies differences in land surface temperature for different urban and natural surfaces. Average temperatures for the CoPP focus areas during the time of the flights showed that tree canopies were the coolest surface type observed during the day. The analysis of street canyon surface temperatures also highlighted the surface cooling effects of tree canopies where a 10 per cent increase in total tree cover (when H:W < 0.8), meant there was around a 1°C reduction in overall canyon land surface temperature during the day (under the study conditions). While the focus here has been on vegetation, state and local governments can use airborne thermal remote sensing data to draw out the role of other surface types on land surface temperature.

The airborne thermal data and relationships presented here represent a specific set of atmospheric conditions under which the data was collected – during an extreme heat event. This means that surfaces would have undergone intense surface heating during the day from clear skies, drawing out large contrasts between surface types. There is likely to be large day to day variability in land surface temperatures spatially resulting from changing synoptic conditions, so the temperatures presented here are most relevant under these types of extreme conditions. This is satisfactory given that it is under these conditions that urban cooling is needed. However, the timing of the data collection also influences the spatial picture, as the ground based observations identified. Had the data been collected in the morning or afternoon, shadows would play a larger part in urban canyon surface temperatures, particularly in north - south oriented canyons. Natural surfaces tend to heat up or cool down quickly (especially non-irrigated grass) compared to urban surfaces, so land surface temperature contrasts are a product of the preceding solar gain and of night-time long-wave radiative loss.

4.2 Key adaptation strategies

While it is well known that increasing vegetation will reduce land surface temperatures, what is not well understood is the amount and location of vegetation required to maximise cooling benefits. Key mitigation strategies are presented below along with recommendations on how best to incorporate green infrastructure into the landscape. This will be built on in the Green Infrastructure Implementation Guide (GIIG) as part of the broader VCCCAR project Responding to the Urban Heat Island: Optimising the Implementation of Green Infrastructure.

1. **Irrigation** – Analysis showed that irrigation of green space was especially effective at reducing land surface temperatures during the day. This emphasises the point of maximising the cooling efficiency of existing green infrastructure first as a priority. For the CoPP focus areas, irrigated grass was on average between 3.58-5.19°C cooler than non-irrigated grass during the day. While the analysis did not compare irrigated and non-irrigated trees, for trees to maintain transpirational cooling and healthy canopies for shade, they must have adequate water supplied to their root systems (Pataki et al., 2011b). During extreme heat events when vapour pressure deficits are high, water availability becomes extremely critical. Stormwater harvesting and water sensitive urban design strategies present an opportunity to retain water in the landscape to maintain healthy vegetation, so it can provide maximum cooling benefits (Coutts et al., 2012). With regards to surface cooling at night, irrigated grass did continue to perform slightly better than non-irrigated grass. In some circumstances, irrigated grass may actually reduce the rate of surface cooling due to the thermal inertia of water (Spronken-Smith and Oke, 1998) and this was observed in average surface temperatures for the Middle Park focus area. Nevertheless, irrigated grass still shows a cooler land surface temperature than urban surfaces, and should be promoted due to the significant daytime benefits and for vegetation health.

2. **Street trees** – Street trees are especially useful in urban cooling due to both transpiration and shading. This was evident in the street canyon analysis, where tree canopy coverage was a dominant vegetation type in the CoPP focus areas. Increasing the tree canopy reduced surface temperatures, and also reduced surrounding road surface temperatures during the day from shading. At night, the benefit of tree cover in reducing land surface temperature was evident but not strong with around 0.4°C reduction in urban canyon surface temperatures (when H:W < 0.8) for a 10 per cent increase in tree cover, while the effect on canyon road surface temperatures was inconclusive. While a dense canopy may restrict night time cooling *within* an urban canyon, the net effect of tree cover at the local scale is one of cooling. As such, street trees should be implemented to mitigate high daytime surface temperatures, as large benefits during the day offset any marginal negative influences at night.

Key factors that influence the cooling effectiveness of street trees include location, size and canopy coverage, planting density, and as outlined above, irrigation management (Pataki et al., 2011a; Shashua-Bar et al., 2010). From the thermal patterns identified in the thermal image the following guidelines were determined to maximise land surface temperature reductions, recognising that only a plan view of the surface can be seen.

East-west oriented streets:

- Street trees should be prioritised for wide streets oriented E-W with a H:W < 0.8
- Maximise canopy coverage on both sides of the street and street centre in wide, open streets with a H:W < 0.8
- Street trees should be prioritised on the south side of E-W oriented streets when H:W > 0.8
- There is little value in implementing street trees in E-W oriented streets with a H:W > 3

North-south oriented streets

- Street trees should be prioritised for wide streets oriented N-S with a H:W < 0.8
- Maximise canopy coverage on both sides of the street and street centre in wide, open streets with a H:W < 0.8
- Street trees should be prioritised for the centre of N-S oriented streets, followed by the east side of the street, then the west side of the street when H:W > 0.8
- There is less value in implementing street trees in N-S oriented streets with a H:W > 3

3. **Open space** – Irrigated and non-irrigated grass areas showed markedly lower land surface temperatures than urban surfaces. From the 30 m grid data, increasing the percentage of grass area, especially irrigated grass area was an effective mechanism for reducing land surface temperature. Larger areas of grass tended to be public open spaces (e.g. parks). At night, although a large proportion of cooling is due to the surface properties, the lack of surrounding buildings means long wave cooling can occur un-inhibited, allowing surface temperatures to reduce further. Open space should be prioritised for locations upwind of areas with high heat exposure (hot-spots) and/or upwind of vulnerable populations.

4. **Green walls** – Green walls are likely to be an effective measure within urban street canyons where space for trees is limited and in urban canyons with a high H:W. The ground based thermography showed that green facades could reduce surface temperatures of building walls compared to the urban materials. The following is suggested from patterns observed in the thermal images and ground based thermography. Green walls should also be irrigated to maximise their cooling potential.

East-west oriented streets:

- Green walls should be prioritised on the south side of E-W oriented streets where space for trees is limited
- Green walls should be prioritised on the south sides of E-W oriented streets with a H:W > 3
- There is little value in implementing green walls on the north side of E-W oriented streets.

North-south oriented streets:

- Green walls should be prioritised on either side of the street where space for trees is limited
- Green walls should be prioritised on the east side of N-S oriented streets
- Green walls should be prioritised on either side of E-W oriented streets with a H:W > 3

5. **Green Roofs** – Green roofs have the capacity to reduce rooftop surface temperatures but are heavily dependent on their design. The ground based thermography of the green roofs highlighted that green roof design is important. Green roofs should be irrigated to maximise evaporative cooling, and to support vegetation health and extensive plant coverage.

4.3 Key limitations of airborne thermal remote sensing

The key limitations with airborne thermal remote sensing have been identified throughout this report and the previous Technical Report, but they are worth reiterating and should be taken into account by those considering the capture of airborne thermal remote sensing.

- Airborne thermal remote sensing presents a picture of the surface temperature rather than canopy layer air temperature. While temperature patterns are broadly similar (e.g. hot-spots) little can be said for the related magnitude of air temperatures.
- Airborne thermal remote sensing presents a plan view of the surface and neglects the three dimensional morphology of the urban landscape, which is important in driving the canopy layer thermal environment.
- Airborne thermal remote sensing must be corrected for emissivity to determine absolute surface temperatures, but is a difficult task and needs further work and research to improve methodologies.
- Airborne thermal remote sensing provides just one snapshot in time. Land surface temperatures at the micro-scale, however, are highly variable temporally, especially during the day. Thermal patterns will therefore vary depending on the time of capture and the meteorological conditions.

- Airborne thermal remote sensing relies heavily on high quality data capture. Data providers must have a clear understanding of the specifications required for thermal data capture. Important things to consider are: time of flights and weather conditions; balancing spatial resolution with capture time; camera specifications; and flight plan. Poor quality data limits the usefulness of the thermal image.
- Auxiliary datasets also need to be of high quality and preferably captured at the same time as the thermal imagery capture or as close to it as possible. This will help eliminate discrepancies between images of areas that have been developed over time (changes in the land surface) and if collected at the same time, will reduce geo-referencing issues.

4.4 Improved approaches for emissivity correction

As stated earlier in this report, the influence of emissivity is complex and makes analysing and interpreting airborne thermal remote sensing data difficult. Neglecting an emissivity correction, or applying an incorrect value for emissivity, can lead to several degrees error in the surface temperature. Sources of error include:

- Misalignment between thermal data and surface data due to different viewing angles of the airborne instruments.
- Shadows which cannot be assigned a value through an automatic supervised classification.
- Limited ability of the thermal camera to accurately capture surfaces as emissivity decreases, becoming compromised below emissivity values of around 0.8.
- Inaccurate classifications of the land surfaces leading to incorrect assignments of emissivity.
- Large variation in values for emissivity in the literature.

Despite these limitations, most of the inaccuracies manifest with regards to rooftops, where identification of roof type is difficult, and emissivity values are most variable. Most emissivity values for ground level surfaces are > 0.9 and show less variability in the literature. As such, a large proportion of the image is likely to be fairly accurate. The rooftops however should be viewed with extreme caution. In this study the focus has been on street canyon temperatures, which excluded the rooftops, partly due to this reason.

To improve the capacity to correct surface temperatures for emissivities, hyper-spectral land surface data should be acquired (Xu et al., 2008) at the same time as the thermal data, using a camera that spans a wide range of the electromagnetic spectrum. This means that classifications of the land surface can use more bands to separate the surface into different types. With some ground truthing, individual rooftop types may be able to be identified, but this would be labour intensive and a correct emissivity value still needs to be applied. There are studies that have used hyper-spectral data with spectral libraries to classify urban areas (Herold, 2003) or with a combination of multiple classifiers (Gamba, 2010). Work has been done in developing a method to classify various different roof materials using hyper-spectral data and feature extraction and this work is showing good potential (Chisense, 2011). However, this increases the cost due to capture and processing of hyper-spectral data. Any auxiliary data sets need to minimise shadowing by flying at solar noon during summer. The best approach would be to gain access to hyper-spectral scanners that collected data in the thermal long-wave band so thermal data can be collected by the same sensor. There are various temperature-emissivity separation algorithms in development in the research field, but these have not been tested at high resolutions in the urban environment (e.g. 1-5 m).

4.5 Contribution of the VCCCAR project

The VCCCAR project has added significant value to the airborne thermal remote sensing data acquired by local councils. The ground based monitoring of surface temperatures enabled a validation of the thermal imagery in the case of CoPP and identified that the quality of the image was acceptable. The project also produced a new thermal image of surface temperatures corrected for emissivity across the CoPP municipality. In the case of CoM, the ground based monitoring stations allowed the assignment of surface temperature values to the digital numbers captured by the thermal camera.

In this report, the VCCCAR project has outlined a methodology for processing and analysing airborne thermal remote sensing data that can be applied by local councils if they choose to obtain data for their respective municipalities. It highlights the strengths and weaknesses of airborne thermal remote sensing and can help state and local governments make a more informed decision about the value of airborne thermal remote sensing.

The outcomes of this report and other products produced in this VCCCAR project have provided valuable information on the effectiveness of urban greening and provide advice on approaches to green infrastructure implementation. If councils wish to map areas of high land surface temperatures within their own municipality, then some form of mapping exercise will be needed. However, the outcomes presented here may be enough for councils to proceed with greening programs regardless, as it outlines what kind of situations lead to excessive surface heating, and when vegetation should be placed to counter this. The Green Infrastructure Implementation Guide will provide further guidance on implementing green infrastructure targeting excess urban heating.

4.6 Alternatives to airborne thermal remote sensing

From this thermal mapping experience, we suggest that the cost of acquiring imagery and the related post-processing required for analysing and interpreting the image makes the value of using airborne thermal remote sensing for high resolution thermal mapping somewhat questionable. Considering the need to access additional data such as hyper-spectral data to allow for correction of emissivity, adds additional costs. Post processing of the data can be very time consuming. The quality of the data will also be dependent on the skill and knowledge of the provider used to conduct the airborne thermal remote sensing. If simply identifying hot-spots is the key purpose, then an unprocessed airborne thermal image will probably suffice.

However, an alternative approach to mapping hot-spots is to acquire satellite data for thermal mapping. Current satellite products provide a coarser resolution product, but still provide the ability to broadly identify hot-spots across the landscape. Two satellite products that provide thermal data include Lansat ETM+ (Enhanced Thematic Mapper) and ASTER (Table 7) at resolutions of 60 m (resampled to 30 m) and 90 m respectively. Landsat is commonly use to map hot-spots in cities (Aniello et al., 1995; Weng, 2009) and provides the highest spatial resolution mapping from space (Tomlinson et al., 2011). Landsat ETM+ thermal data is free from the USGS website, and is available as raw data or corrected for atmospheric effects so as to reduce post processing time. Only daytime images at the acquisition time are available.

GIS officers within state government and local council should have the necessary skills to acquire and process Landsat ETM+ data, or could do so with some additional training. This is likely to be simpler than what is required for the post processing of the high resolution airborne thermal remote sensing. In combination with the guidance on implementing green infrastructure from this project and using Landsat ETM+ data for the thermal mapping probably provides a more cost-effective approach to mapping hot-spots than high resolution airborne thermal remote sensing. The selected approach does come down to the intended use of the product, and the higher resolution mapping may be required in some cases, for example in this project, for analysing within canyon land surface temperatures, and the identification of individual surface features (e.g. trees). A new Landsat satellite is due for launch in 2013.

Table 7: Specifications of satellite remote sensing products (from Tomlinson et al., 2011)

Sensor	Landsat ETM+	ASTER
Satellite	Landsat 7	Terra
Spatial resolution	60m*	90m
Orbital frequency	16 days	Twice daily
Image acquisition	11:00 local time	Request only
TIR spectral bands (μm)	(6) 10.4-12.5	(10) 8.125–8.475 (11) 8.475–8.825 (12) 8.925–9.275 (13) 10.25–10.95 (14) 10.95–11.65
Data avilable	1999 onwards#	1999
Website	http://pubs.usgs.gov/fs/2010/3026/	http://asterweb.jpl.nasa.gov/index.asp

*** Can be resampled to 30 m.**
 # Landsat ETM data from 2003 onwards are impaired due to failure of the scan line corrector and mean only approximately 80% of each scene is captured.

While collection of thermal data may be interesting for government or industry, the purpose of this research project was to draw out key adaptation strategies. Local Councils, for instance, should be able to use the information provided here and in the Green Infrastructure Implementation Guide to help guide investment in urban greening without the need for costly mapping exercises. Local practitioners should have a good understanding of their local environment and be able to prioritise street tree implementation and other green initiatives based on the principles outlined from this research.

4.7 Future research

While the thermal data has helped identify some key approaches to implementing green infrastructure, a more robust set of guidelines could be developed through the use of micro-scale climate models of the street canyon. This would allow for testing a range of street canyon orientations and H:Ws to identify what spatial arrangements produce cooler outdoor thermal environments. A micro-scale urban climate model that also includes vegetation would also then allow testing of a range of greening scenarios. While this study identified a H:W of 0.8 as a cut off point for prioritising tree cover implementation, micro-scale modelling will allow an assessment of a more diverse set of canyon arrangements. Also, this study has targeted reductions in land surface temperature and not air temperature: a micro-climate model could provide guidance on implementation of green infrastructure to mitigate high air temperatures. Monash University is presently pursuing this research direction.

As highlighted, further research is needed concerning approaches to improving the emissivity correction of high resolution thermal imagery.

More research is needed on within-canyon effects of trees on complete (3D) land surface temperatures and air temperatures at night. While it is clear that long-wave radiative cooling is restricted below tree canopies at night, the effect of this on air temperatures at the micro-scale is less well known. Certainly, previous research has demonstrated links between low sky view factor and urban heating at night of canopy layer air temperatures. The cause is predominantly placed on the buildings, yet vegetation cover can also contribute to a low sky view factor. Research is needed on the net effects of vegetation that link the micro-scale and the local scale effects of vegetation, where trees may lead to slightly warmer air temperatures within the canyon, but provide an overall reduction in the local scale air temperatures due to reduced daytime heat storage.

Finally, research into the relationship between surface temperatures and internal building energy performance is needed. As highlighted, little can be drawn from airborne thermal remote sensing about building energy efficiency. Further research is needed on the influence of different greening strategies on internal building climates and energy use in the southern hemisphere, as the focus of this study has been on the external thermal environment.

5. Acknowledgments

This project was funded by the Victorian Centre for Climate Change Adaptation Research (VCCCAR). Sincere thanks to the City of Port Phillip and the City of Melbourne for making available the thermal imagery for the project, along with supporting GIS data layers. Thanks to Dr. Nick Williams, Dr. Steve Livesley and Professor Jason Beringer for assistance in data collection. Acknowledgement is also made to Dr. Shobhit Chandra for advice provided to local councils on specifications for the thermal data capture. Thanks to Monash City Council for permission to monitor the green roof at the council premises.

References

AKBARI, H. & KONOPACKI, S. 2005. Calculating energy-saving potentials of heat-island reduction strategies. *Energy Policy*, 33, 721-756.

ANIELLO, C., MORGAN, K., BUSBEY, A., NEWLAND, L. 1995. Mapping microurban heat islands using Landsat TM and a GIS. *Computers and Geosciences* 21: 965–967

ARYA, P. S. (2001) Introduction to Micrometeorology, Great Britain, Academic Press

BÄRRING, L., MATTSSON, J. O. & LINDQVIST, S. 1985. Canyon geometry, street temperatures and urban heat island in malmö, sweden. *Journal of Climatology*, 5, 433-444.

BOWLER, D. E., BUYUNG-ALI, L., KNIGHT, T. M. & PULLIN, A. S. 2010. Urban greening to cool towns and cities: A systematic review of the empirical evidence. *Landscape and Urban Planning*, 97, 147-155.

BRACK, C. L. 2002. Pollution mitigation and carbon sequestration by an urban forest. *Environmental Pollution*, 116, S195-S200.

CHISENSE, C., HAHN, M. AND ENGELS, J. 2011. Classification of Roof Materials using Hyperspectral Data. *Applied Geoinformatics for Society and Environment*. Nairobi: AGSE.

COUTTS, A. M., DALY E., MEINIG, R., HARRIS, R., NICE, K. 2012. Heat mitigation effects of four experimental roof rigs. (In preparation)

COUTTS A, HARRISR 2011. Technical Report: Airborne Thermal Remote Sensing for Analysis of the Urban Heat Island, *Victorian Centre for Climate Change Adaptation Research.*

COUTTS, A. M., TAPPER, N. J., BERINGER, J., LOUGHNAN, M. DEMUZERE, M. 2012. Watering our cities: The capacity for Water Sensitive Urban Design to support urban cooling and improve human thermal comfort in the Australian context. *Progress in Physical Geography* (In Press)

DOUSSET, B. & GOURMELON, F. 2003. Satellite multi-sensor data analysis of urban surface temperatures and landcover. *ISPRS Journal of Photogrammetry and Remote Sensing*, 58, 43-54.

ELIASSON, I. 1992. Infrared thermography and urban temperature patterns. *International Journal of Remote Sensing*, 13, 869-879.

FLETCHER, T. D., DELETIC, A., MITCHELL, V. G. & HATT, B. E. 2008. Reuse of Urban Runoff in Australia: A Review of Recent Advances and Remaining Challenges. *J. Environ. Qual.*, 37, S-116-S-127.

GAMBA, P., DELL'ACQUA, F.,BAKOS, K. AND LISINI, G. 2010. Information extraction from hyper-spectral data in urban areas using contextual information and classifier fusion. Hyperspectral Workshop. Frascati, Italy: European Space Agency.

GILL, S. E., HANDLEY, J. F., ENNOS, A. R. & PAULEIT, S. 2007. Adapting Cities for Climate Change: The Role of the Green Infrastructure. *Built Environment,* 33, 115-133.

GRIMMOND, C. S. B., ROTH, M., OKE, T. R., AU, Y. C., BEST, M., BETTS, R., CARMICHAEL, G., CLEUGH, H., DABBERDT, W., EMMANUEL, R., FREITAS, E., FORTUNIAK, K., HANNA, S., KLEIN, P., KALKSTEIN, L. S., LIU, C. H., NICKSON, A., PEARLMUTTER, D., SAILOR, D. & VOOGT, J. 2010. Climate and More Sustainable Cities: Climate Information for Improved Planning and Management of Cities (Producers/Capabilities Perspective). *Procedia Environmental Sciences,* 1, 247-274.

HARMAN D. L. (1994) Global Physical Climatology, United States, Academic Press

HEROLD, M., GARDNER, M.E. AND ROBERTS, D.A 2003. Spectral Resolution Requirements for Mapping Urban Areas. *IEEE Transactions on Geoscience and Remote Sensing,* 41.

KOTTMEIER, C., BIEGERT, C. & CORSMEIER, U. 2007. Effects of Urban Land Use on Surface Temperature in Berlin: Case Study, ASCE.

LIU, K. K. Y. & MINOR, J. 2005. Performance evaluation of an extensive green roof. *Greening rooftops for sustainable communities.* Washington DC.

LO, C. P., QUATTROCHI, D. A. & LUVALL, J. C. 1997. Application of high-resolution thermal infrared remote sensing and GIS to assess the urban heat island effect. *International Journal of Remote Sensing,* 18, 287-304.

LUNDHOLM, J., MACIVOR, J. S., MACDOUGALL, Z. & RANALLI, M. 2010. Plant Species and Functional Group Combinations Affect Green Roof Ecosystem Functions. *PLoS ONE,* 5, e9677.

MACIVOR, J. S., RANALLI, M. A. & LUNDHOLM, J. T. 2011. Performance of dryland and wetland plant species on extensive green roofs. *Annals of Botany,* 107, 671-679.

McMICHAEL, A. J., WOODRUFF, R. E. & HALES, S. 2006. Climate change and human health: present and future risks. *Lancet,* 367, 859-869.

MORRIS, C. J. G. & SIMMONDS, I. 2000. Associations between varying magnitudes of the urban heat island and the synoptic climatology in Melbourne, Australia. *International Journal of Climatology,* 20, 1931-1954.

NIACHOU, A., PAPAKONSTANTINOU, K., SANTAMOURIS, M., TSANGRASSOULIS, A. & MIHALAKAKOU, G. 2001. Analysis of the green roof thermal properties and investigation of its energy performance. *Energy and Buildings,* 33, 719-729.

NICHOLLS, N., SKINNER, C., LOUGHNAN, M. & TAPPER, N. 2008. A simple heat alert system for Melbourne, Australia. *International Journal of Biometeorology,* 52, 375-384.

NOWAK, D. J.. CRANE, D. E., STEVENS, J. C. 2006. Air pollution removal by urban trees and shrubs in the United States. Urban Forestry and Urban Greening 4:115-123.

OFFERLE, B., ELIASSON, I., GRIMMOND, C. & HOLMER, B. 2007. Surface heating in relation to air temperature, wind and turbulence in an urban street canyon. *Boundary-Layer Meteorology,* 122, 273-292.

OKE, T. R. 1987. *Boundary Layer Climates,* Great Britain, Cambridge University Press.

PATAKI, D. E., CARREIRO, M. M., CHERRIER, J., GRULKE, N. E., JENNINGS, V., PINCETL, S., POUYAT, R. V., WHITLOW, T. H. & ZIPPERER, W. C. 2011a. Coupling biogeochemical cycles in urban environments: ecosystem services, green solutions, and misconceptions. *Frontiers in Ecology and the Environment,* 9, 27-36.

PATAKI, D. E., MCCARTHY, H. R., LITVAK, E. & PINCETL, S. 2011b. Transpiration of urban forests in the Los Angeles metropolitan area. *Ecological Applications,* 21, 661-677.

QUATTROCHI, D. A., RIDD, M.K. 1994. Measurement and analysis of thermal energy responses from discrete urban surfaces using remote sensing data. *International Journal of Remote Sensing,* 15, 1991-2022.

ROSENZWEIG, C., SOLECKI, W. D., COX, J., HODGES, S., PARSHALL, L., LYNN, B., GOLDBERG, R., GAFFIN, S., SLOSBERG, R. B., SAVIO, P., WATSON, M. & DUNSTAN, F. 2009. Mitigating New York City's Heat Island: Integrating Stakeholder Perspectives and Scientific Evaluation. *Bulletin of the American Meteorological Society,* 90, 1297-1312.

ROTH, M., OKE, T. R. & EMERY, W. J. 1989. Satellite-derived urban heat islands from three coastal cities and the utilization of such data in urban climatology. *International Journal of Remote Sensing,* 10, 1699-1720.

SAARONI, H., BEN-DOR, E., BITAN, A. & POTCHTER, O. 2000. Spatial distribution and microscale characteristics of the urban heat island in Tel-Aviv, Israel. *Landscape and Urban Planning,* 48, 1-18.

SHASHUA-BAR, L. & HOFFMAN, M. E. M. E. 2004. Quantitative evaluation of passive cooling of the UCL microclimate in hot regions in summer, case study: urban streets and courtyards with trees. *Building and Environment,* 39, 1087-1099.

SHASHUA-BAR, L., ODED, P., ARIEH, B., DALIA, B. & YARON, Y. 2010. Microclimate modelling of street tree species effects within the varied urban morphology in the Mediterranean city of Tel Aviv, Israel. *International Journal of Climatology,* 30, 44-57.

SPRONKEN-SMITH, R. A. & OKE, T. R. 1998. The thermal regime of urban parks in two cities with different summer climates. *International Journal of Remote Sensing,* 19, 2085 - 2104.

SPRONKEN-SMITH, R. A., OKE, T. R. & LOWRY, W. P. 2000. Advection and the surface energy balance across an irrigated urban park. *International Journal of Climatology,* 20, 1033-1047.

STONE, B. & RODGERS, M. O. 2001. Urban form and thermal efficiency - How the design of cities influences the urban heat island effect. *Journal of the American Planning Association,* 67, 186-198.

STREUTKER, D. R. 2002. A remote sensing study of the urban heat island of Houston, Texas. *International Journal of Remote Sensing,* 23, 2595-2608.

STREUTKER, D. R. 2003. Satellite-measured growth of the urban heat island of Houston, Texas. *Remote Sensing of Environment,* 85.

TOMLINSON, C. J., CHAPMAN, L., THORNES, J. E. & BAKER, C. 2011. Remote sensing land surface temperature for meteorology and climatology: a review. *Meteorological Applications,* 18, 296-306.

UPMANIS, H. & CHEN, D. 1999. Influence of geographical factors and meteorological variables on nocturnal urban-park temperature differences - a case study of summer 1995 in Goteborg, Sweden. *Climate Research,* 13, 125-139.

WENG, Q. 2009. Thermal Infrared remote sensing for urban climate and environmental studies: Methods, applications, and trends. *Journal of Photogrammetry and Remote Sensing* 64, 335-344.

WENG, Q., LU, D. & SCHUBRING, J. 2004. Estimation of land surface temperature–vegetation abundance relationship for urban heat island studies. *Remote Sensing of Environment,* 89, 467-483.

WONG, N. H., CHEN, Y., ONG, C. L. & SIA, A. 2003. Investigation of thermal benefits of rooftop garden in the tropical environment. *Building and Environment,* 38, 261-270.

WONG, N. H., KWANG TAN, A. Y., CHEN, Y., SEKAR, K., TAN, P. Y., CHAN, D., CHIANG, K. & WONG, N. C. 2010. Thermal evaluation of vertical greenery systems for building walls. *Building and Environment,* 45, 663-672.

XU, W., WOOSTER, M. J. & GRIMMOND, C. S. B. 2008. Modelling of urban sensible heat flux at multiple spatial scales: A demonstration using airborne hyperspectral imagery of Shanghai and a temperature–emissivity separation approach. *Remote Sensing of Environment,* 112, 3493-3510.

Appendix A – Calculation of City of Melbourne land surface temperatures

As indicated, some complications arose during the capture of the City of Melbourne airborne thermal remote sensing data. The flight plan was not clearly communicated between the service providers and the project research partners and as such, the flight was conducted in a time efficient manner – rather than a progressive capture (e.g. from west to east). The original data was captured in a non-sequential way and this created a thermal image that had obvious stripes on it, showing large differences in temperatures over the same land cover types. This was due to the cooling of the surface over the couple of hours between capturing neighbouring stripes. This was compounded by a misunderstanding of the time it would take to capture the entire image. The project partners were of the understanding the flight would take be completed in two hours, but it was completed in three and a half hours, which meant surface temperatures could have cooled substantially. The flight was also meant to be conducted from 12am–2am on 24 February, but appears it was completed from 10.45pm to 2.15am. Due to the stripes in the image, the raw data could not be used in a meaningful way and needed to be corrected.

The image was provided to an outside company with suitable software and the data was radiometrically corrected so that the brightness values of the image were normalised. However an issue with this new image is that all the original data numbers representing each pixel and its corresponding temperature value were changed. As such the original look-up table to assign surface temperatures could not be used. The new image was essentially a set of digital numbers that were higher if surface temperatures were high, but no temperature value could be assigned.

To assign a temperature value to the digital values, ground control points established by Monash University were used. At the time of flight there were seven ground control points located in the City of Melbourne. These ground control points covered a range of land surface types including concrete, water and grass. Polygons were created to represent the same ground area on the image as that observed by the ground control points. The mean pixel value was then calculated for each polygon area. These mean pixel values were then plotted against the temperature value recorded at 1am for the ground control points. A linear relationship was assumed between the pixel values and temperature recorded from ground control points. This assumption of a linear relationship was concluded by looking at the relationship between pixel value and temperature of the City of Port Phillip image. This linear relationship was then applied to the whole image to create temperature values for the thermal image.

Due to the way the temperature values have been calculated there are some issues with the accuracy of the image. With regards to the radiometric balancing of the original data, this means that the pixel numbers are not the original values. Also, the use of only seven ground control points might not give an accurate relationship between the pixel values and surface temperatures. There might not be a linear relationship between the two and as a result this relationship might not be appropriate. With these uncertainties the temperature values that are represented as estimation and not the absolute temperature values that were present at the time of capture. This example demonstrates the need for clear communication with service providers capturing the thermal data, and some of the difficulties surrounding capture of high quality data and the value of ground control points and validation. Nevertheless, the final image still provides for the main purpose of the image capture of identifying hot-spots and using the image as a valuable communication tool around the influence of the surface on urban climate development.

Appendix B – Assessment of supervised classification

A 500 random point confusion matrix of the whole CoPP supervised classification after some manual editing. The confusion matrix shows an overall accuracy of 88.4 per cent. It also has a Kappa coefficient of 0.86 which shows a strong agreement of the classification

# Plots	Concrete	Irrigated Grass	Non Irrigated Grass	Road	Shadow	Tile Roof	Tin Roof	Trees	Water	Totals	User's Accuracy
Concrete	20							1		21	95.24
Irrigated grass		6						1		7	85.71
Non irrigated grass			45	1				6		52	86.54
Road	4			96	5	1				106	90.57
Shadow				1	50	3				54	92.59
Tile roof	3			4	7	46	1	2		63	73.02
Tin roof	4		2		3	1	98	1		109	89.91
Trees		2		2	3			68		75	90.67
Water									13	13	100.00
Totals	31	8	47	104	68	51	99	79	13	500	
Producer's accuracy	64.52	75.00	95.74	92.31	73.53	90.20	98.99	86.08	100.00		**88.40**

Kappa	
Part A	442
Part B	37945
N	500
K	0.86

Appendix C – Thermal images for City of Melbourne (24 February 2012) and City of Port Phillip (25 February 2012)

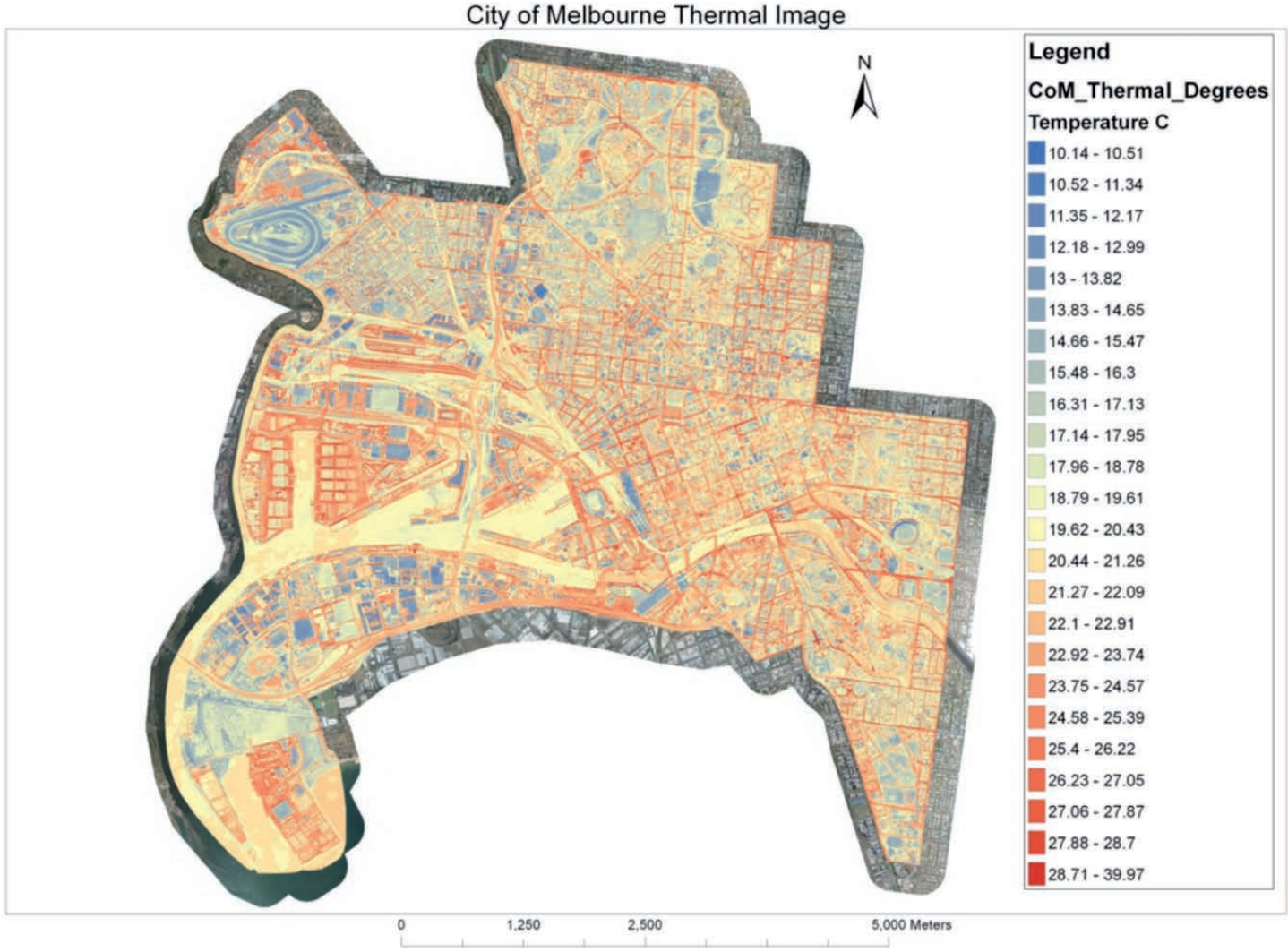

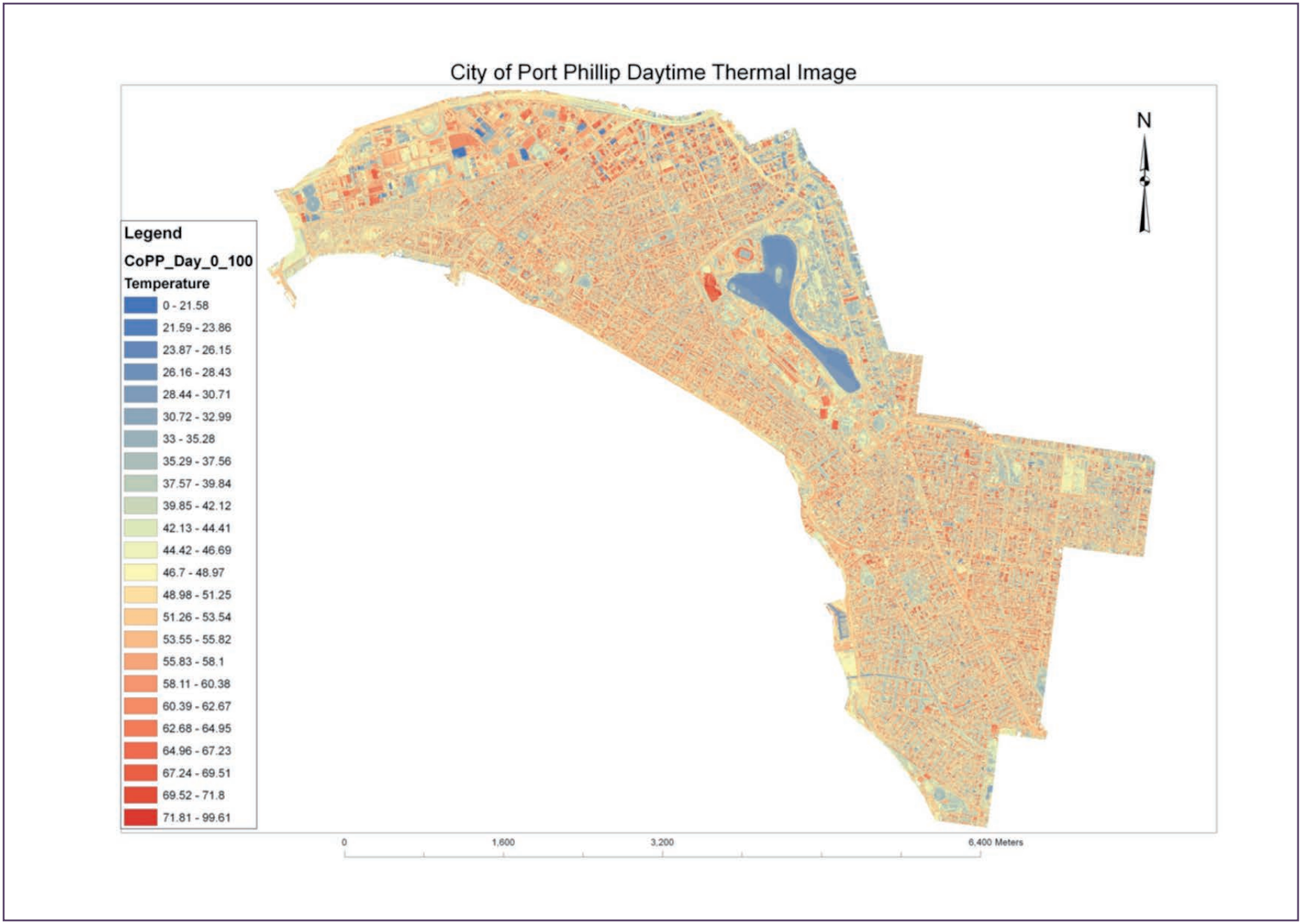
City of Port Phillip Daytime Thermal Image
N
Legend
CoPP_Day_0_100
Temperature
0 - 21.58
21.59 - 23.86
23.87 - 26.15
26.16 - 28.43
28.44 - 30.71
30.72 - 32.99
33 - 35.28
35.29 - 37.56
37.57 - 39.84
39.85 - 42.12
42.13 - 44.41
44.42 - 46.69
46.7 - 48.97
48.98 - 51.25
51.26 - 53.54
53.55 - 55.82
55.83 - 58.1
58.11 - 60.38
60.39 - 62.67
62.68 - 64.95
64.96 - 67.23
67.24 - 69.51
69.52 - 71.8
71.81 - 99.61
0
1,600
3,200
6,400 Meters

Appendix D – Air temperature transects for City of Melbourne (24 February 2012) and City of Port Phillip (25 February 2012)

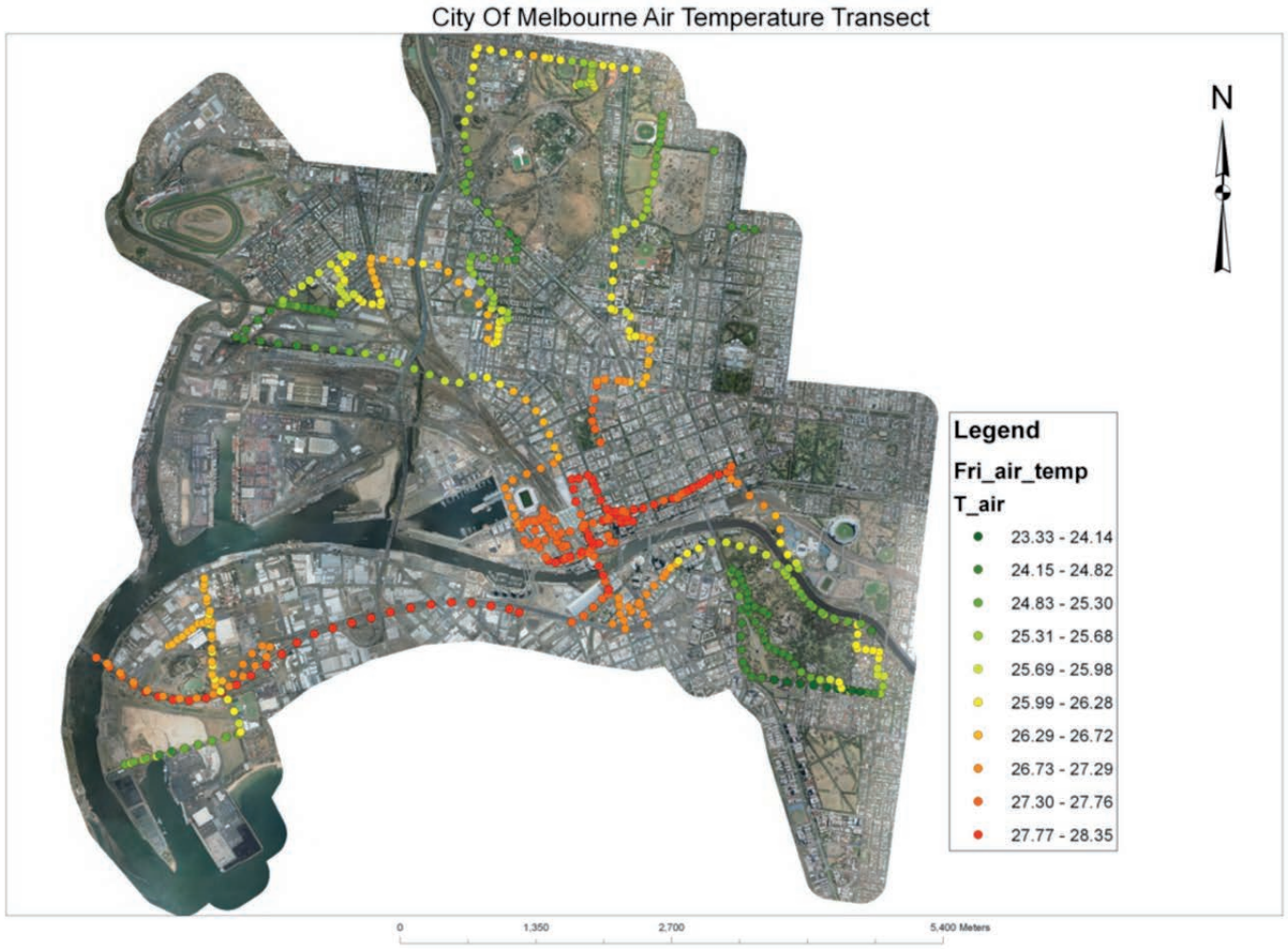

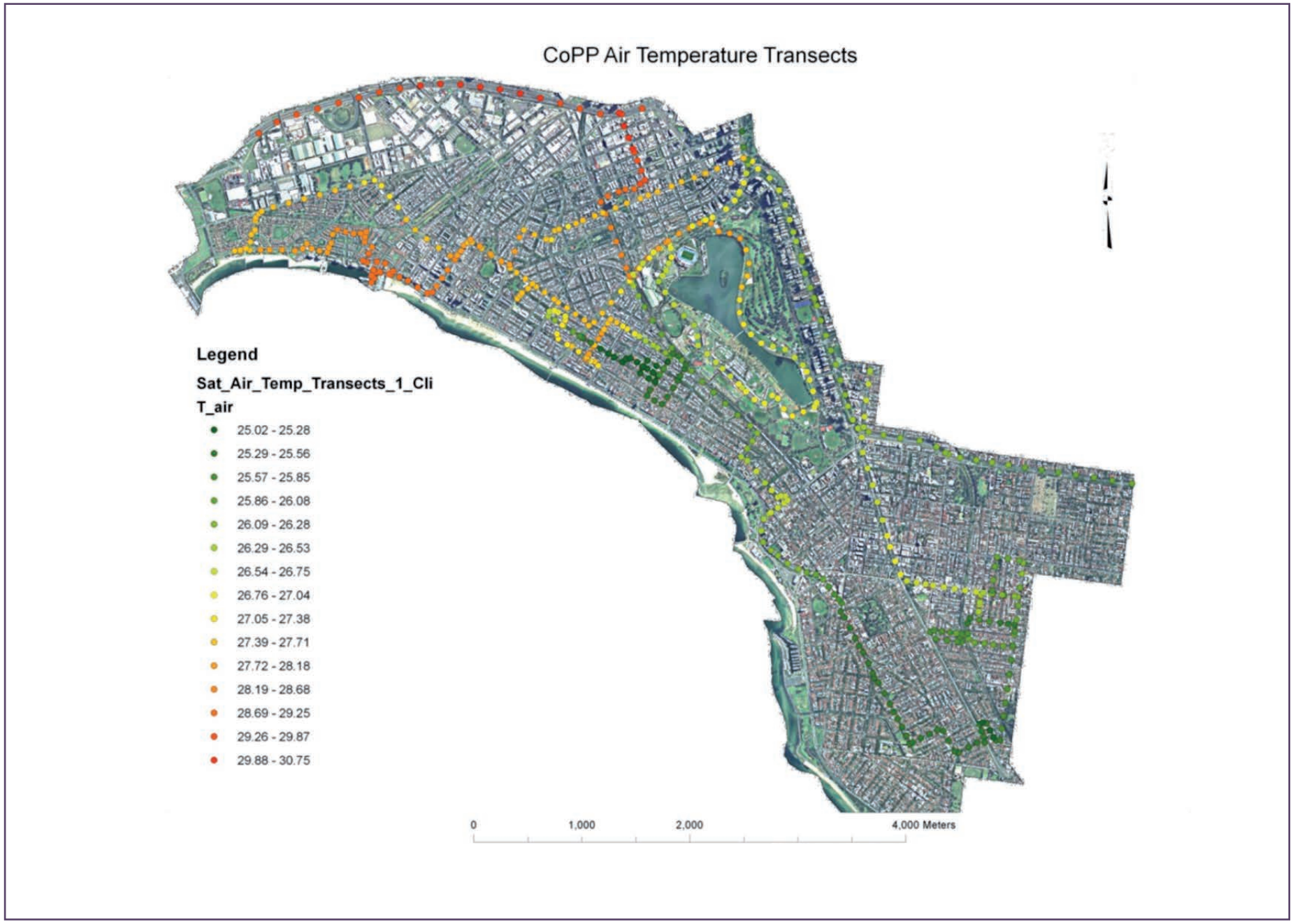
CoPP Air Temperature Transects
Legend
Sat_Air_Temp_Transects_1_Cli
T_air
25.02 - 25.28
25.29 - 25.56
25.57 - 25.85
25.86 - 26.08
26.09 - 26.28
26.29 - 26.53
26.54 - 26.75
26.76 - 27.04
27.05 - 27.38
27.39 - 27.71
27.72 - 28.18
28.19 - 28.68
28.69 - 29.25
29.26 - 29.87
29.88 - 30.75
0
1,000
2,000
4,000 Meters

Disclaimer: The views expressed herein are not necessarily the views of the State of Victoria, and the State of Victoria does not accept responsibility for any information or advice contained within.

© Copyright Victorian Centre for Climate Change Adaptation Research and Monash University 2013.
VCCCAR Publication ISBN: 978 0 7340 4840 0
Document available from VCCCAR website at:
www.vcccar.org.au/publications

Layout and design by Inprint Design
www.inprint.com.au